



# The Reservoir Temperature Estimator (RTEst): A Multicomponent Geothermometry Tool

May 2024

*Changing the World's Energy Future*

Carl D. Palmer, Robert W. Smith, Ghanashyam Neupane, Travis L McLing



**DISCLAIMER**

This information was prepared as an account of work sponsored by an agency of the U.S. Government. Neither the U.S. Government nor any agency thereof, nor any of their employees, makes any warranty, expressed or implied, or assumes any legal liability or responsibility for the accuracy, completeness, or usefulness, of any information, apparatus, product, or process disclosed, or represents that its use would not infringe privately owned rights. References herein to any specific commercial product, process, or service by trade name, trade mark, manufacturer, or otherwise, does not necessarily constitute or imply its endorsement, recommendation, or favoring by the U.S. Government or any agency thereof. The views and opinions of authors expressed herein do not necessarily state or reflect those of the U.S. Government or any agency thereof.

# **The Reservoir Temperature Estimator (RTEst): A Multicomponent Geothermometry Tool**

**Carl D. Palmer, Robert W. Smith, Ghanashyam Neupane, Travis L McLing**

**May 2024**

**Idaho National Laboratory  
Idaho Falls, Idaho 83415**

**<http://www.inl.gov>**

**Prepared for the  
U.S. Department of Energy  
Under DOE Idaho Operations Office  
Contract DE-AC07-05ID14517**

# The Reservoir Temperature Estimator (RTEst): A Multicomponent Geothermometry Tool

Carl D. Palmer<sup>(1)\*</sup>, Robert W. Smith<sup>(2,3)</sup>, Ghanashyam Neupane<sup>(3,4)</sup>, and Travis L. McLing<sup>(3,4)</sup>

<sup>1</sup>Geography and Geological Sciences, University of Idaho, Moscow, Idaho, USA (Adjunct);

<sup>2</sup>Earth and Spatial Sciences, University of Idaho, Moscow, Idaho, USA

<sup>3</sup>Center for Advanced Energy Studies, Idaho Falls, Idaho, USA;

<sup>4</sup>Idaho National Laboratory, Idaho Falls, Idaho, USA;

\*Corresponding Author, email: palmerc7@comcast.net

## Abstract

The Reservoir Temperature Estimator (RTEst) is a multicomponent geothermometry tool for estimating reservoir geochemical parameters including reservoir temperature, CO<sub>2</sub> fugacity, mass of water lost or gained, and a reaction factor. It estimates these parameters and their associated uncertainties by minimizing a loss function that is the weighted sum of squares of the saturation indices of a user-selected set of minerals believed to be equilibrated with the reservoir fluid. RTEst accomplishes these estimates by combining the geochemical modeling capabilities of The Geochemist's Workbench® with the optimization/parameter estimation resources of PEST®. An included interface aids the user in selecting plausible mineral phases to comprise the loss function and calculates their weighting factors. The working principles of RTEst are described and its efficacy is illustrated by presenting results of its application to various geothermal fields for which the conditions are known. These examples show RTEst can account for the alteration of ascending reservoir fluid by mineral (calcite) re-equilibration with changes in temperature, reconstruct waters with CO<sub>2</sub> loss, correct for the deficit of water and other volatiles (CO<sub>2, gas</sub>, H<sub>2</sub>S<sub>gas</sub>) from boiling, and determine the amount of mixing of thermal and non-thermal waters. RTEst can use data with basis species below detection limit, missing, or unreliable either by assuming equilibrium with a controlling mineral (fixed-analyte method) or by treating the analyte concentration as an optimization parameter. The inverse of variance weighting method included in RTEst provides more representative results than either the normalization or unit weighting methods. The ability of RTEst to calculate reservoir temperatures, gas fugacity, and mixing fractions demonstrates its usefulness as a tool for evaluating geothermal systems.

## Introduction

A major barrier to the deployment of renewable geothermal energy technology is the high exploration and development costs (U.S. Department of Energy, 2011). For example, Glacier Partners (2009) estimated that 55% of the cost of a 35 MW geothermal project is in exploration, drilling, and design. Expanding the penetration of geothermal into energy markets requires the development of more cost-effective and reliable prospecting tools to help minimize financial risks. Recent advances in geochemical analyses and modeling allow for improved accuracy of solute geothermometry and may provide the industry with such a cost-effective prospecting tool.

Solute geothermometry is a tool for estimating deep reservoir temperature from the geochemical composition of water samples collected from hot springs and shallow thermal wells. The approach can be traced back to White et al. (1956) who suggested that silica concentrations could indicate reservoir temperatures. Solute geothermometry is based on two fundamental assumptions: 1) the attainment of temperature-dependent chemical equilibrium between the water and minerals (primarily alteration minerals) at the deep reservoir conditions; and 2) preservation of chemical composition of the reservoir fluid during its ascent to the surface (e.g., Fournier et al., 1974). Most geothermometry is conducted using “traditional” approaches where one or a few chemical components (dissolved silica or cation ratios, gases, isotopes) are used to estimate reservoir temperatures (Williams et al., 2008). Common approaches include SiO<sub>2</sub>, Na-K, Na-K-Ca, Na-K-Ca-Mg, Na-Li, and K-Mg geothermometers (e.g., Fouillac and Michard, 1981; Fournier, 1977; Fournier and Potter, 1979; Fournier and Rowe, 1966; Fournier et al., 1979; Fournier and Truesdell, 1973; Giggenbach, 1988; Truesdell and Fournier, 1977). Over one hundred such traditional geothermometers are summarized elsewhere (Cioni and Marini, 2020; Powell and Cumming, 2010; Verma et al., 2008). While the application of these traditional geothermometers can provide valuable insights, they suffer from several limitations: i) no straightforward method to assess the accuracy and uncertainty of the temperature prediction of any individual geothermometer, ii) absence of methods to assess which geothermometers provide the best estimate of reservoir temperature, iii) inability of most geothermometers to determine the impact of physical and chemical process that alter solute concentrations and thus reservoir temperature estimates, and iv) assumption of mineral equilibrium that may not apply. These limitations result in diverse temperature estimates from the various geothermometers, decreasing their reliability as a geothermal prospecting tool.

An improved geothermometric approach addressing these issues is a multicomponent method that uses many chemical constituents measured in water samples (Michard and Roekens, 1983; Reed and Spycher, 1984). The method has been applied by several researchers at various geothermal systems (e.g., D'Amore et al., 1987; Hull et al., 1987; Tole et al., 1993). This approach uses a geochemical speciation model to calculate the saturation states of individual minerals for a measured water chemistry as a function of temperature to identify a common reservoir temperature at which the water is in equilibrium with likely reservoir minerals. The key drawback to this method is that it is a graphical approach that requires subjective estimation of the clustering of the saturation index (SI) curves. A substantial improvement of this multicomponent approach was the development of the Get software package (Spycher et al., 2014). GeoT uses an optimization approach with a choice of four loss functions that provides a more objective estimate of the intersection of the mineral saturation indexes and the associated equilibrium reservoir temperature.

We have developed a geothermometry tool, the Reservoir Temperature Estimator (RTEst), based on the multicomponent approach with inverse geochemical optimization capability (Mattson et al., 2015; Palmer, 2014). In this paper, we describe the working principles of RTEst and demonstrate its efficacy by presenting results of RTEst applied to various case studies for which reservoir conditions are understood. The natural geothermal case study settings include the Breitenbush Hot Springs in central Oregon, USA,

the Ojo Caliente Hot Springs system, and thermal features in the Boundary Creek area in Yellowstone National Park, Wyoming, USA, and the thermal wells in Iceland. These geothermal fields with known reservoir temperatures offer excellent test cases for evaluating the applicability and reliability of RTEst for reservoir temperature estimation.

## Approach

Basic concepts of multicomponent geothermometry are described by others (e.g., Bethke, 2008; Reed and Spycher, 1984; Spycher et al., 2014). Simply stated the method involves calculating saturation state (as defined below) of a near-surface thermal water sample as a function of temperature with respect to possible reservoir minerals. The temperature of the deeper and hotter associated geothermal reservoir can be graphically estimated as the temperature at which the multiple mineral species deemed likely to be present in the reservoir are in equilibrium with the solution composition. Challenges of a strictly graphical approach includes the selection an equilibrium reservoir mineral assemblage(s) consistent with the thermodynamic phase rule and defining the equilibrium states for real non-idealized systems with water chemistries subject to measurement error. The RTEst tool automates the process of estimating reservoir temperature and other geochemical parameters including CO<sub>2</sub> fugacity ( $f_{\text{CO}_2}$ ), mass of water lost or gained, and total Al concentration and their associated uncertainties by minimizing a loss function ( $L_2$ ) that is the weighted sum of squares of the saturation indices ( $SI_k$ ) of a user-selected set of minerals hypothesized to be at equilibrium with reservoir fluids:

(1)

where  $w_k$  is the weighting factor for the  $k$ th mineral,  $SI_k = \log [Q_k/K_k(T)]$ , and  $Q_k$  and  $K_k(T)$  are the ion activity product and temperature-dependent equilibrium constant for  $k$ th mineral and  $m$  is the number of minerals in the user-selected set. This approach recognizes that the value of  $SI_k$  for a solution in equilibrium with the  $k$ th mineral will have a value of zero while positive and negative values indicate supersaturation and undersaturation, respectively.

There are three options for weighting factors in RTEst: unit weights, normalization, and inverse of variance. Proper weighting is important because in nonlinear models, such as multicomponent geothermometry, heteroscedasticity can cause biased and inconsistent parameters and an inconsistent covariance matrix (e.g., Greene, 2018). Because of this inherent heteroscedasticity coupled with analytical uncertainties associated with measured water chemistries, we prefer inverse of variance weighting.

The inverse of variance method assumes

(2)

where  $\sigma_k$  is the variance in the saturation index of the  $k$ th mineral. More specifically, we assume that this variance is the conditional variance in the saturation index given the value of the equilibrium constants used in calculating the chemical speciation and the saturation index ( $s^2(SI_k|K_i)$ ). This conditional variance obtained through a propagation of error calculation accounts for the stoichiometry of the mineral and the analytical uncertainty of the associated basis species and is expressed as a standard deviation for the SI:

(3)

where  $C_i$  is the concentration of the  $i$ th basis species,  $\sigma_i$  is the standard deviation of  $C_i$ ,  $(\sigma_i/C_i)$  is the coefficient of variation of the basis species (i.e., the analytical error) and  $n_b$  is the number of basis species. The  $\psi_i$  parameter includes contributions of activity coefficient terms and is close to unity for most ions over the temperature range of 0° to 300°C and for ionic strength up to 3 molal (Mattson et al., 2015).

Normalized weighting is a special case of the inverse of variance method in which the analytical error for all basis species is equal to  $\psi_i/\ln(10)$ , the activity of water is unity, and the activity of  $H^+$  has no error. This is the weighting method that was employed by Cooper et al. (2013) and is similar to the methods employed by Wolery (1979) and Reed (1982; 1998). This method considers the different stoichiometries in the minerals by using

(4)

where  $n_c$  is the number of basis species excluding  $H^+$  and  $H_2O$ , and  $\nu_{i,k}$  is the stoichiometric coefficient of  $i$ th basis species in the  $k$ th mineral phase. While this method accounts for stoichiometry, it does not allow for differences in the uncertainty of various analytes. As a result, this weighting method is inferior to the preferred inverse of variance weighting method for real-world water samples with variable analyte-specific uncertainties.

Unit weighting implicitly assumes that a numerical value of  $SI$  for a mineral with one basis species (e.g., quartz– $SiO_2$ ) represents the same distance from equilibrium for the same  $SI$  value of a clay mineral (e.g., nontronite– $SiO_2$ ,  $Al^{3+}$ ,  $Fe^{3+}$ , and exchangeable cations) that has many basis species. Such an assumption would bias the result toward equilibrium with the nontronite over equilibrium with quartz. In addition, unit weighting does not account for influence of the arbitrary choice of stoichiometry for minerals (e.g.,  $CaMg(CO_3)_2$  vs.  $Ca_{0.5}Mg_{0.5}CO_3$ ) on the magnitude (but not the sign) of  $SI$  values. From a statistical perspective, unit weighting results in heteroscedasticity since the variance in the saturation states depend on stoichiometry (Equation (3)) and are therefore different for each mineral. For these reasons, we do not recommend using unit weights.

The saturation state of a mineral can be described using the number of standard deviations from saturation ( $n_{SD}$ ):

(5)

The advantage of using  $n_{SD}$  rather than  $SI$  is that it considers mineral stoichiometries and analytical uncertainties of basis species involved in mineral-fluid reactions as a measure of distance from equilibrium. Geothermometric models based on different assumptions (e.g., different mineral suites) are evaluated by comparing the average of the absolute values of the  $n_{SD}$  of all the minerals used in calculating the loss function ( $\Phi$ ).

## Mineral Selection

The application of RTEst requires the user to select a set of minerals that are likely to be equilibrated with the geothermal fluids in the reservoir. Mineralogical analysis of samples from borehole cores and cuttings would be a great aid in selecting this assemblage, however, such information is rarely available during early exploratory work. However, there is often information about the general lithology of the suspected reservoir and one can infer potential mineralogy from this lithology. As a result, selecting which minerals that should be members of that set represents an area of continuing uncertainty for systems for which direct mineralogical characterizations are unavailable. In these cases, the choice of minerals depends on several factors (e.g., Browne, 1978) including the reservoir lithology, water type and temperature. Because geothermal systems are often equilibrated with common alteration mineral assemblages rather than the primary reservoir lithology (e.g., Bethke, 2008; Giggenbach, 1988), a generalized approach for identifying equilibrium controlling minerals across a range of reservoir types is possible. This approach is based on a review of studies that identify alteration mineral assemblages that form when hot water interacts with reservoir minerals (e.g., Schwartz, 1959) and is implemented in RTEst as described by Palmer et al. (2014). Cioni and Marini (2020) provide additional information on the selection of mineral

phases in hydrothermal systems.

Based on an analysis of 48 geothermal systems representing all major geologic environments typically associated with geothermal activity, Palmer et al. (2014) suggested 16 mineral assemblages classified on a hierarchical categorization based on five lithologies (tholeiitic, calc-alkaline, silicic, siliciclastic, and carbonates), three temperature regimes (low, 50-150 °C; moderate, 150-300 °C; and high, >300 °C), and two water types (neutral and acidic). This hierarchical categorization and their associated mineral assemblages are described by Palmer et al. (2014) and shown in Figure 1 and Table 1, respectively. Determining secondary minerals by this method has limitations. For example, suggestions of “zeolite” or “smectite” are general terms that do not identify the specific zeolite or smectite that could be present. Nonetheless, this approach can prove useful in assisting the user in choosing mineral suites likely to be present in the geologic setting being considered.

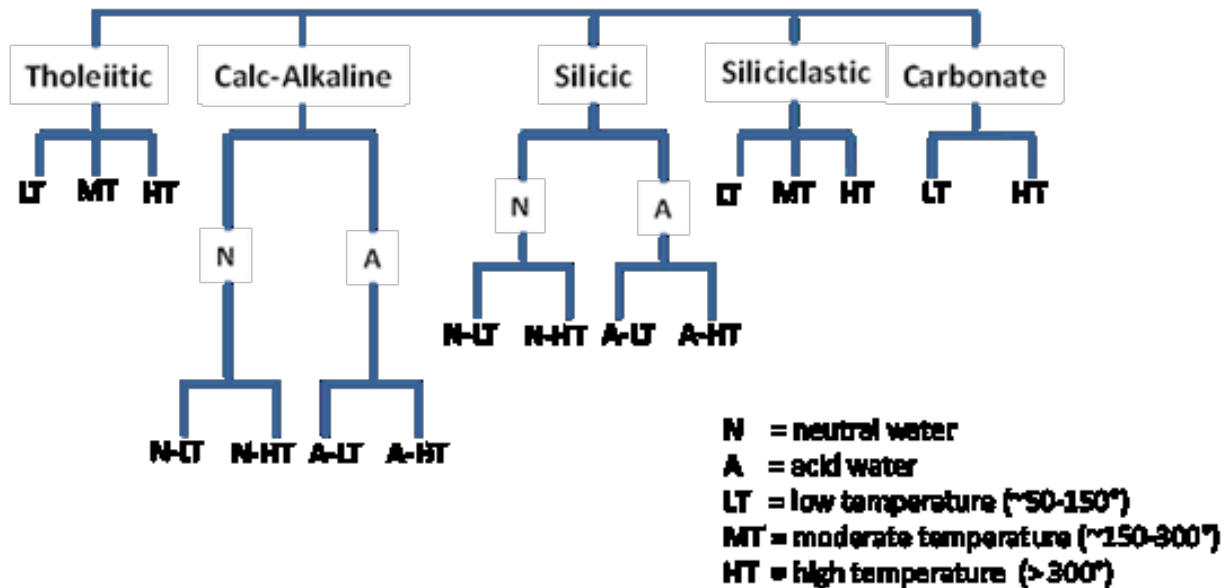


Figure 1. Hierarchical listing of influencing parameters and assemblage groups (Palmer et al., 2014).

Table 1. Representative geothermal alteration mineral assemblages for hierarchical classification shown in Figure 1 (Palmer et al., 2014). (T=tholeiitic, CA=calc-alkaline, S=silicic, SC=siliciclastic, C=carbonate, N = neutral, A = acidic, LT = low temperature, MT = moderate temperature, HT = high temperature).

<b>Assemblage ID</b>	<b>Minerals present</b>
T-LT	Chalcedony ± quartz + zeolites + smectite + calcite ± limonite + pyrite + anhydrite
T-MT	Quartz + wairakite + albite + titanite + epidote + prehnite + mixed layer clay (chlorite/smectite) ± smectite ± chlorite + calcite + pyrite + anhydrite
T-HT	Quartz + wairakite + albite + wollastonite ± clinopyroxene + actinolite + titanite + garnet + epidote + prehnite + chlorite + calcite + pyrite + anhydrite
CA-N-LT	Zeolites ± cristobalite ± quartz + smectite ± chlorite + calcite + hematite ± goethite + pyrite + anhydrite ± barite + native sulfur
CA-N-HT	Quartz + wairakite + albite + adularia + clinopyroxene + actinolite + titanite + epidote + prehnite ± biotite + chlorite + illite + calcite + pyrite + anhydrite ± barite ± halides
CA-A-LT	Amorphous silica ± cristobalite + kaolinite + smectite ± montmorillonite + calcite + hematite ± goethite + pyrite + alunite ± anhydrite + native sulfur
CA-A-HT	Quartz + albite + clinopyroxene + actinolite + titanite + epidote + biotite/prehnite + chlorite + illite + calcite + pyrite + anhydrite ± halides
S-N-LT	Quartz + zeolites + adularia + smectite/kaolinite/montmorillonite + calcite + pyrite ± anhydrite
S-N-HT	Quartz + albite ± potassium feldspar + epidote + sericite/muscovite + chlorite + calcite + pyrite ± anhydrite
S-A-LT	Cristobalite + opal ± quartz + zeolites + adularia + smectite/kaolinite/montmorillonite/mixed layer clays ± hematite + sulfides + alunite ± barite
S-A-HT	Quartz + albite ± potassium feldspar + epidote + sericite/muscovite + montmorillonite/kaolinite/chlorite + sulfides + alunite ± barite ± halides
SC-LT	Potassium feldspar + albite + mixed layer clay (illite/smectite) ± chlorite + calcite ± ankerite/dolomite + hematite + pyrite + anhydrite
SC-MT	Quartz + wairakite + potassium feldspar + albite + titanite + epidote + chlorite + calcite + hematite + pyrite + anhydrite
SC-HT	Quartz + potassium feldspar + albite ± clinopyroxene + actinolite + titanite + garnet + epidote + biotite + calcite + hematite + pyrite
C-LT	Feldspar ± quartz + calcite ± ankerite/dolomite + hematite
C-HT	Feldspar ± quartz + clinopyroxene + actinolite + titanite + epidote + biotite ± chlorite + calcite

## Program Structure

### Optimization

RTEst is built as an interface program that combines The Geochemist's Workbench® (GWB) geochemical modeling capabilities and optimization/parameter estimation algorithms of PEST® (Figure 2). The GWB software package comprises several modules for managing compositional data for waters, balancing chemical reactions, producing activity-activity diagrams, conducting aqueous speciation and mass transfer calculations. In addition, the package includes interactive graphing capability facilitating the production of standard and customized plots of results. Of importance here is the GWB React module, details of which can be found in (Bethke and Yeakel, 2014a, b). RTEst was originally developed under Release 10 of GWB but has been used with Release 12 and Release 15. The calculations are supported by included thermodynamic data bases. We used the default *thermo* (based on the Lawrence Livermore National Laboratory (LLNL) dataset which was modified by adding the two micas celadonite ( $\text{KMgAlSi}_4\text{O}_{10}(\text{OH})_2$ ) and celadonite-Fe ( $\text{KFeAlSi}_4\text{O}_{10}(\text{OH})_2$ ) and the zeolite stilbite ( $\text{CaAl}_2\text{Si}_7\text{O}_{25}\text{H}_{14}$ ). In addition, the temperature ranges for  $\text{CaSO}_4^0$ ,  $\text{MgSO}_4^0$ , and  $\text{MgCO}_3^0$  were extended from 200 to 300°C. The thermodynamic data for the modifications were obtained from the SUPCRTBL software package with its standard database (Zimmer et al., 2016). PEST® is a generalized software suite for parameter estimation and uncertainty analysis that can be applied to any model through interfaces with its input and output files (<https://pesthompage.org/>). RTEst currently uses version 17.3 of the PEST® suite. Details of the program can be found in the user's manuals (Doherty, 2018a, b) while the statistical methods are described in Doherty (2015).

RTEst requires two user files: 1) a GWB React file and 2) a RTEst input file. The react file contains the concentration of analytes for the water for which the geothermometric calculations are being made. In addition, this file may contain instructions for altering the water chemistry, such as adding reactants. The RTEst input file includes number, type, initial guess, and ranges of the optimized parameters and a list of minerals included in the assemblage along with their weighting factors. When RTEst is run, it generates PEST® files based on the user input file. It then calls PEST®, which reads these files and initializes the optimization. PEST® then calls the RTEst Interface routine, which sends updated parameter estimates to GWB React program and retrieves the resultant saturation indices for the mineral suite. This process continues iteratively until the loss function is minimized at which point PEST® generates several output files. Chief among them is the PEST® \*.MTT file that includes optimized values for reservoir temperature and other optimized geochemical parameters and their associated uncertainties. Additional statistical information includes the parameter covariance and correlation coefficient matrices and the normalized eigenvectors and eigenvalues of the covariance matrix that can be used to understand the interactions between the optimized parameters and the contribution of each of these factors to the result. Doherty (2015) describes the statistical methods and the associated statistical parameters and their interpretation.

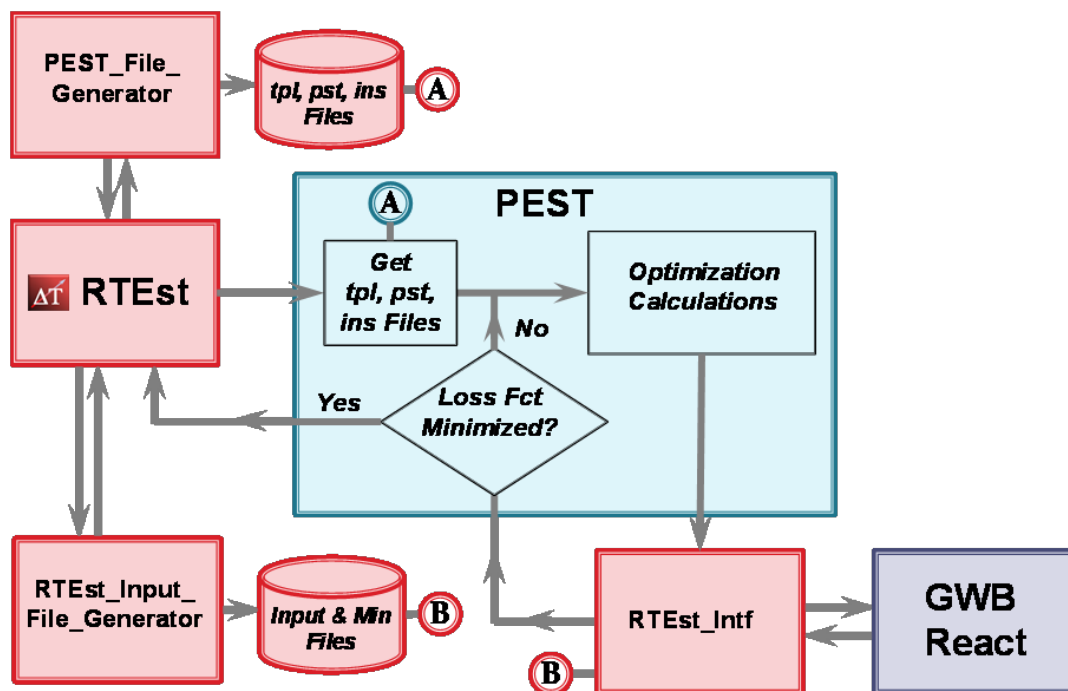


Figure 2. General flow diagram for RTest.

### RTest Input File Generator

Although the RTest input file can be constructed manually in any text editor, it is more convenient to use the input file generator to 1) ensure proper calculation of the weighting factors, 2) aid in the selection of minerals to be included in the loss function, and 3) ensure the selected mineral assemblage does not violate the Gibbs phase rule. The RTest Input File Generator opens as a tabbed form where the user can simply check the parameters being optimized and fill in text boxes for the names of the file, and initial guess and boundaries for the optimized parameters. In the Mineral Assemblage tab (Figure 3), the user can select the lithology, water type (acidic or neutral pH), and expected temperature range. When the “Update Mineral List” button is clicked, a subset of the minerals in the database that are compatible with the choices of lithology, water type, and temperature range are displayed. The user can then choose which of these are used in the loss function by checking the appropriate boxes and clicking the “Add” button. The independence of the choice of minerals can be determined by clicking on the “Phase Rule Check” button. In the “Weighting” tab, the user can choose the weighting method (inverse of variance, normalization, unit values) before creating the input file in the “Finish” tab.

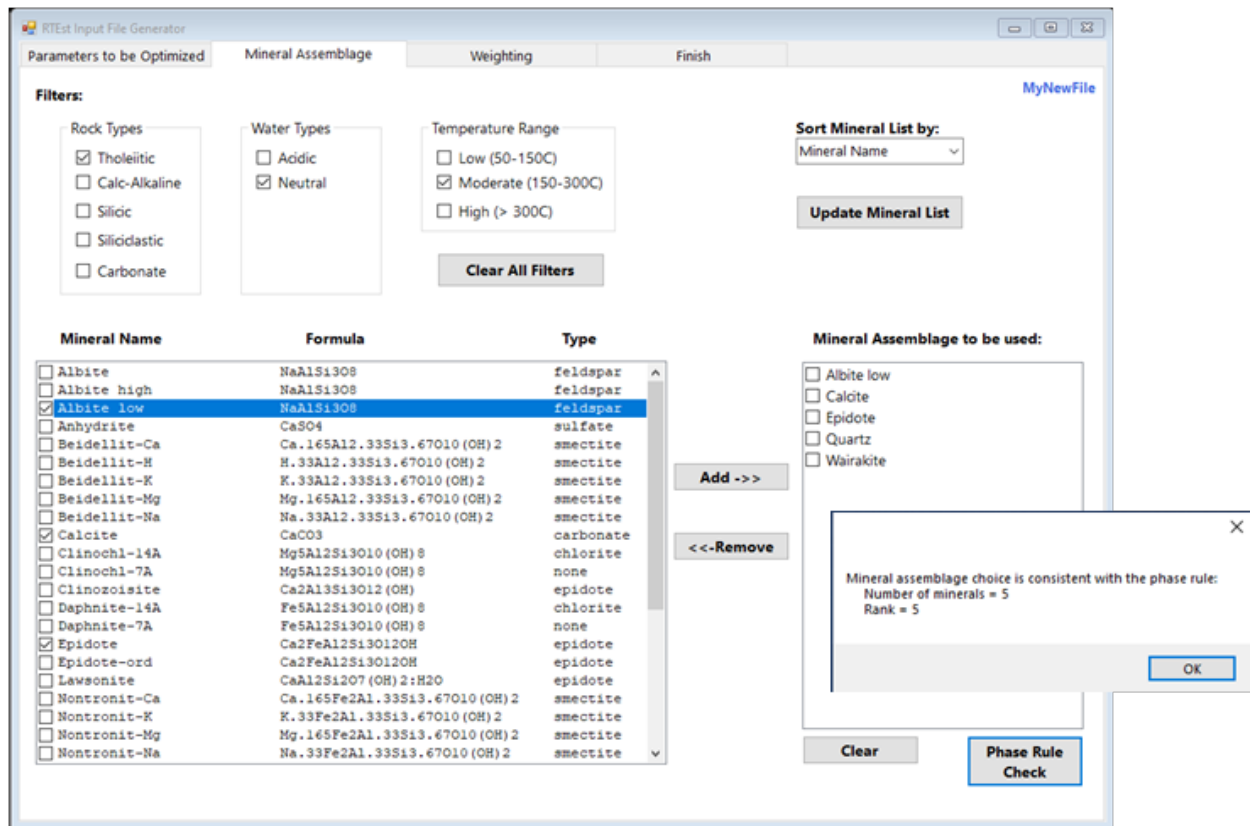


Figure 3. Mineral Assemblage tab in the RTEst Input File Generator subprogram.

## Examples

### Estimate of Reservoir Temperature with Calcite Equilibrium

Geothermometric calculations are often based on the assumption that the ascending fluid maintains solute concentrations like those in the reservoir. However, if the rate of reaction exceeds the rate of fluid transport, the thermal fluid may re-equilibrate at lower temperatures before it reaches the surface. Such re-equilibration is particularly likely for calcite, whose dissolution rate is sufficiently rapid that, as the reservoir fluid cools, it may dissolve to maintain equilibrium (Bethke, 2008; Palandri and Reed, 2001) altering  $\text{Ca}^{2+}$  and total inorganic carbon (TIC) concentrations and pH from those of the geothermal reservoir. Malkemus et al. (2021) made this assumption for the springs and wells at Breitenbush Hot Springs in the Cascade Mountains of central Oregon, U.S.A. Their sample W1 was from a 151-m deep well with an outflow temperature of 86°C. The fluid is equilibrated with calcite ( $SI = +0.04$ ) at the outflow temperature, suggesting a minimal loss of  $\text{CO}_2(\text{gas})$  as this fluid ascended from the reservoir. Using RTEst, we calculated the reservoir temperature by two different methods: A) assuming no calcite reaction and B) assuming re-equilibration of calcite with temperature. In both cases, we used the measured laboratory pH (at 23°C) and measured solute concentrations as the initial fluid except for  $\text{Al}^{3+}$  and Fe(III) which were calculated from K-feldspar and goethite equilibrium, respectively. For case A, the mineral suite used in the loss function comprises chalcedony, laumontite, heulandite, celadonite, epidote, and calcite. The choice of these minerals is based on observed mineralogy in a 2,457-meter-deep well drilled ~3 km southeast of Breitenbush Hot Springs (Barger, 1994). For case B, calcite is excluded from the loss function, but it is allowed to re-equilibrate with changes in temperature.

A plot of  $n_{SD}$  versus temperature (Figure 4) for case A shows convergence of the curves at  $127.9 \pm 6.9^\circ\text{C}$ . The  $n_{SD}$  show a relatively large range of values ( $\text{avg}|n_{SD}| = 2.05$  for minerals included in the loss function) at the optimized temperature with the  $n_{SD}$  of chalcidony and laumontite  $> 2$  and the  $n_{SD}$  of calcite being  $> 6$  even though it is included in the loss function.

As expected for case B, the calculated reservoir  $\text{Ca}^{2+}$  and TIC concentrations ( $1.64$  and  $2.73 \text{ mmol kg}^{-1}$ ) are less than the discharge concentrations ( $2.22$  and  $3.30 \text{ mmol kg}^{-1}$ ) indicating calcite dissolution during ascension of the fluid. This re-equilibration results in a calculated reservoir temperature ( $139.5 \pm 2.6^\circ\text{C}$ ) with a smaller uncertainty and a temperature that is closer to the maximum down-hole temperature measured in the SUNEDCO 58-28 drill hole ( $141^\circ\text{C}$ ). The  $n_{SD}$  for the minerals in the loss function have a smaller range of saturation states ( $\text{avg}|n_{SD}| = 0.72$ ). This approach also provides lower uncertainties than traditional and sulfur isotope geothermometry, which yield temperatures ranging from  $129$  to  $202^\circ\text{C}$  (Mariner et al., 1993).

Besides the minerals included in the loss function, illite, kaolinite, mordenite-K, clinoptilolite-K also appear to be equilibrated with the posited reservoir fluid and have been observed in nearby outcrops and drill holes but with lower frequency (Malkemus et al., 2021). Electron microscopy of clays in the area (Bargar and Oscarson, 1997) suggests some smectites have compositions intermediate between smectite-high-Mg-Fe and smectite-low-Mg-Fe, while others are closer to saponite. The geothermometric analysis suggests that the reservoir fluid is equilibrated with both smectites. This example shows that RTEst can calculate accurate reservoir temperatures even when a portion of the geochemical signature is altered by subsequent mineral reaction and can provide evidence for other minerals potentially equilibrated with the reservoir fluid.

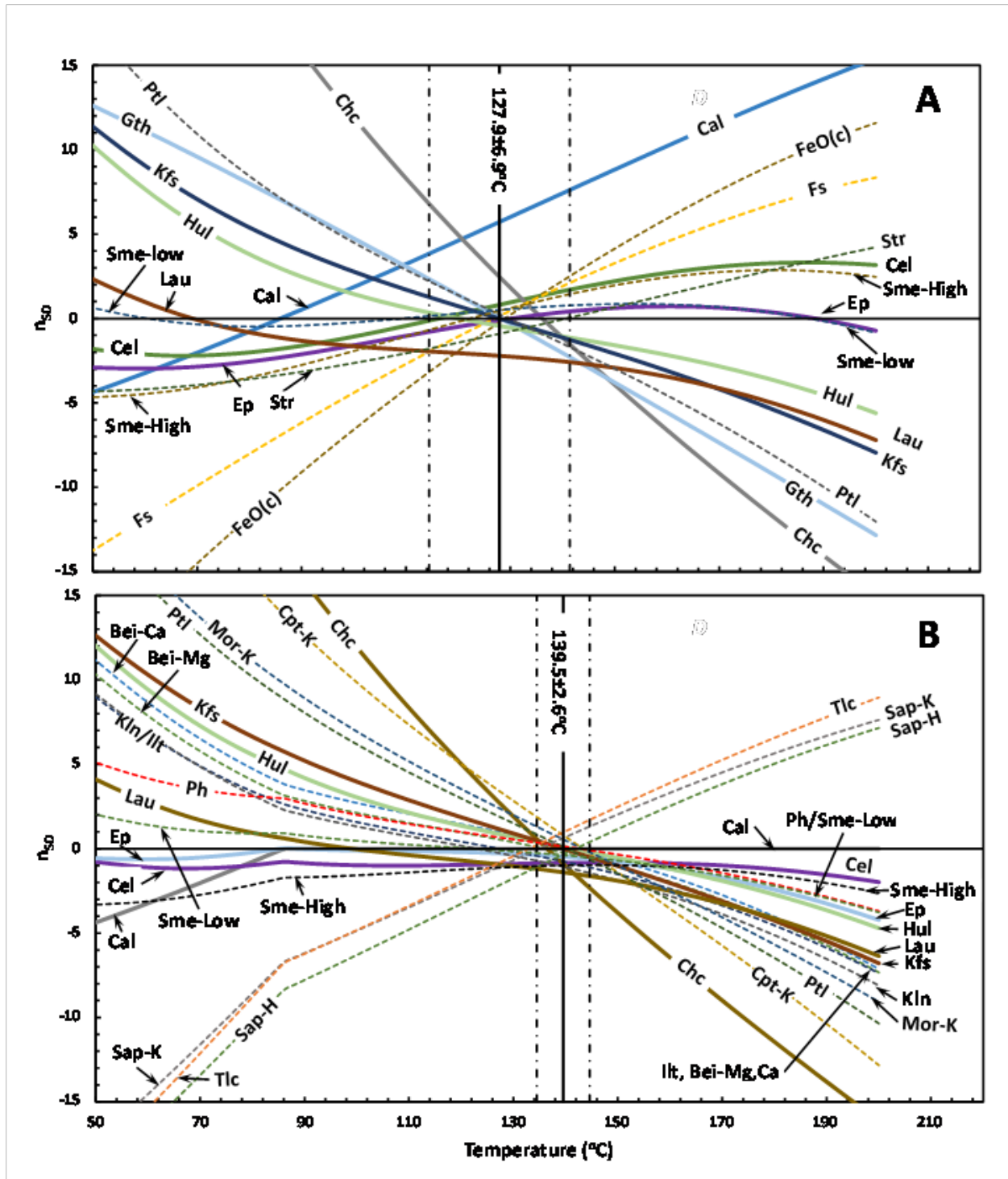


Figure 4, Plot of  $n_{SD}$  versus temperature for selected minerals for sample W1 at Breitenbush Hot Springs, central Oregon (A) using calcite in the loss function and (B) assuming re-equilibration with calcite with changes in temperature. Solid lines denote minerals included in the loss function or presumed to be equilibrated in the fluid. Dashed lines denote additional minerals with  $|n_{SD}| < 1$  at the optimized temperature. For the plot,  $Al^{3+}$  and  $Fe(III)$  concentrations held constant at values calculated at the optimum temperature. Mineral abbreviations are listed in the Appendix 1.

## Accounting for CO<sub>2</sub> Loss

### Reconstructing Waters with CO<sub>2</sub> Loss

As geothermal waters are discharged at the surface, they often lose volatile constituents, particularly CO<sub>2,gas</sub>. Accurate geothermometry requires that the chemical composition of the water be reconstructed by accounting for this volatile loss. At the Breitenbush Hot Springs in central Oregon, Malkemus et al. (2021) observed that springs have the same solute (e.g., Na<sup>+</sup> and Cl<sup>-</sup>; Figure 5) concentrations as deep wells except for TIC, which were lower and pH values, which were higher in the springs. These observations are consistent with the spring waters being derived from the same geothermal source as the wells but having lost CO<sub>2,gas</sub>. The 180Deg spring has a discharge temperature of 82°C, which is slightly less than the temperature in W1 (86°C). Because the deeper waters are equilibrated with calcite, which is prevalent in the underlying rocks, we assume that the spring should also be equilibrated with calcite. The amount of CO<sub>2,gas</sub> that must be added back to reconstruct the water chemistry can be calculated using RTEst by allowing CO<sub>2,gas</sub> to be a reactant and optimizing the amount of reaction (i.e., the GWB<sup>®</sup> parameter reactTimes) using calcite as a mineral in the loss function. An alternative approach, optimizing the log(*f*CO<sub>2</sub>) rather than a CO<sub>2,gas</sub> reactant, yielded identical results. The calculated TIC, pH, and *f*(CO<sub>2</sub>) in the reconstructed fluid are all within the expected uncertainty of the values obtained for sample W1 (Figure 5). Uncertainty cannot be associated with this calculation because only a single mineral is used in the loss function. Nonetheless, this example demonstrates RTEst's usefulness in reconstructing waters that have lost volatile constituents.

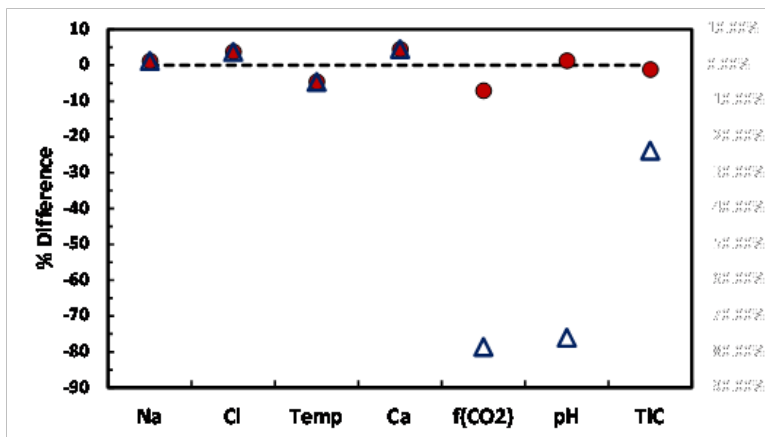


Figure 5. Percent difference for several geochemical parameters between samples W1 and 180Deg Spring at Breitenbush, Oregon before (triangles) and after (circles) adding back CO<sub>2(gas)</sub> to 180Deg Spring to bring the solution to equilibrium with calcite.

### Consistency

Although the previous example shows that one can account for CO<sub>2,gas</sub> outgassing in reconstructing reservoir conditions for a single sample, the question arises of the consistency of the results when multiple samples are collected. The Ojo Caliente Hot Springs in the Lower Geyser Basin of Yellowstone National Park (YNP) in Wyoming, USA provides an opportunity to demonstrate such consistency since all the samples emanate from a single source but are altered by varying degrees of CO<sub>2,gas</sub> outgassing, cooling, and evaporation.

The Lower Geyser Basin comprises an impermeable near-surface zone (<30 m to 76 m) below which is the first aquifer (reservoir) which may transition further down to deeper aquifers. White et al. (1975) recorded a bottom-hole (157 m) temperature of ca. 201-204°C in the drill-hole Y-2 in the Lower Geyser

Basin. Similarly, White et al. (1975) also report a temperature up to 196°C for the lower sections (150 m-156 m) of a nearby drill-hole (Y-3).

Thermal water from Ojo Caliente discharges as slightly alkaline Na-Cl type water to a pool, then flows through a network of channels to the Firehole River (Figure 6). The U.S. Geological Survey (e.g., Ball et al., 2002; Ball et al., 2010; Ball et al., 1998; McCleskey et al., 2014; White et al., 1975) has sampled this hot spring multiple times. We have selected water chemistry data of eight samples collected from the exit point of the pool to the end of the longest flow channel (Figure 6). Temperature of the water decreases from 91.9°C at the exit (sample 101) to 50.5°C (sample 112) near the Firehole River (Figure 7). The decrease in calculated  $\log(f\text{CO}_2)$  from -1.74 to -2.95 with the concomitant increase in pH from 7.6 to 8.47 along the flow channel (Figure 7) results from  $\text{CO}_2$  loss to the atmosphere (Nordstrom et al., 2005).

We applied RTEst to all samples to optimize reservoir temperature and  $\text{CO}_2$  fugacity. The mineral assemblage comprising albite, calcite, potassium feldspar, quartz, and zoisite was selected using the RTEst mineral assemblage filters (silicic + siliciclastic rocks, moderate temperature, and neutral water) and local geologic information (Bargar and Beeson, 1981; White et al., 1975). There is a significant correlation between  $\text{Cl}^-$  concentrations and distance ( $r^2 = 0.950$ ;  $p(\text{slope}) = 8.7\text{E-}5$ ) so sample concentrations were corrected for evaporation, however, this correction is small ( $< 2.3\%$ ) and has little impact on the results. The convergence of the  $n_{SD}$  of the minerals in the loss function yielded optimized temperatures, as illustrated for sample S101 (Figure 8). In addition, siderite, ripidolite-14A, beidellite (-Na, -Ca, -Mg) and nontronite (-Na, -K, -Mg) appear to be equilibrated with the fluids in the reservoir, however, we are not aware of their identification in nearby drill holes. The minerals presumed here as being equilibrated at the optimized temperature are similar to minerals used by Nordstrom et al. (2019) in their multicomponent geothermometric calculations. The RTEst temperature estimates obtained across the Ojo Caliente samples are similar (208-212°C), and close to the measured bottom hole temperatures (202.5°C) in the nearby wells (Figure 9) but are higher than the estimated temperature ( $172 \pm 15^\circ\text{C}$ ) by Nordstrom et al. (2019). Estimated reservoir temperatures across the samples ( $193.0 \pm 2.9$ ,  $181.2 \pm 2.2$ , and  $139.3 \pm 0.5^\circ\text{C}$ ) for the quartz, quartz with steam formation, and Na/K geothermometers of Arnórsson et al. (1983b) also underestimate the reservoir temperature. These results from Ojo Caliente Hot Springs demonstrate the efficacy of RTEst in accurately estimating reservoir temperatures and reconstructing TIC concentration for sampled thermal waters that have undergone varying amounts of cooling and  $\text{CO}_2$  outgassing.

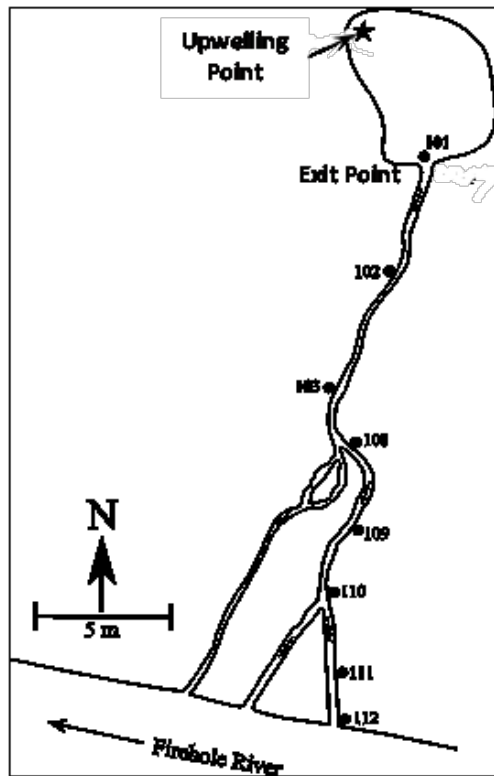


Figure 6. Map of the Ojo Caliente Hot Spring in Lower Geyser Basin, YNP (modified from Ball et al., 1998). Numbers denote sampling locations along the overflow channel.

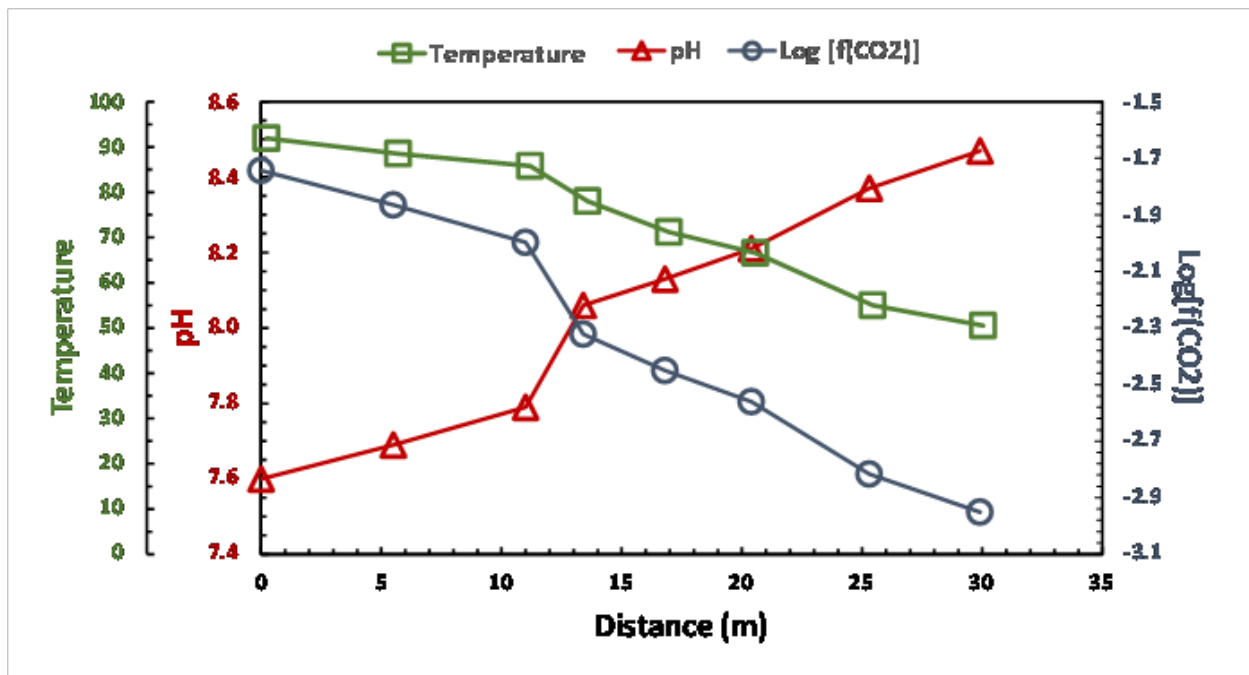


Figure 7. Measured temperature, pH, and  $\log(f\text{CO}_2)$  of samples from Ojo Caliente Spring in YNP. Data from Ball et al. (1998).

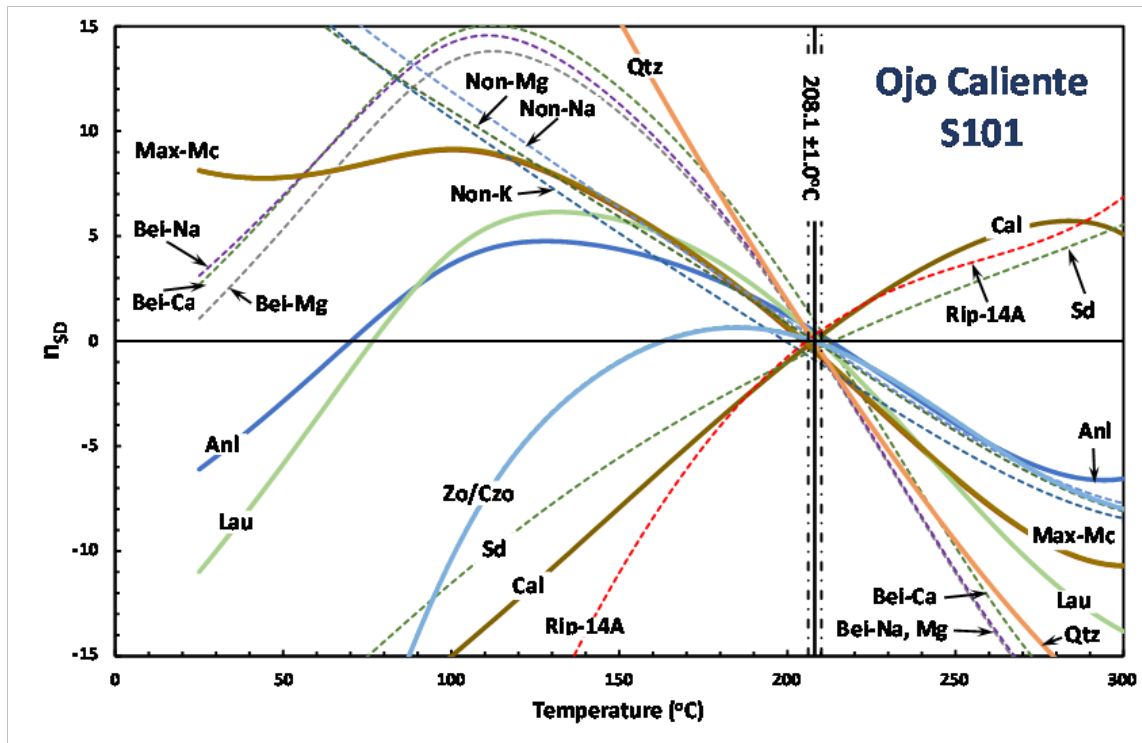


Figure 8. Plot of  $n_{SD}$  versus temperature for selected minerals for sample S101 at Ojo Caliente Hot Springs, YNP. Solid lines denote minerals included in the loss function. All included minerals have  $|n_{SD}| < 1$  at the optimized temperature. Based on data from Ball et al. (1998). Mineral abbreviations are listed in Appendix 1.

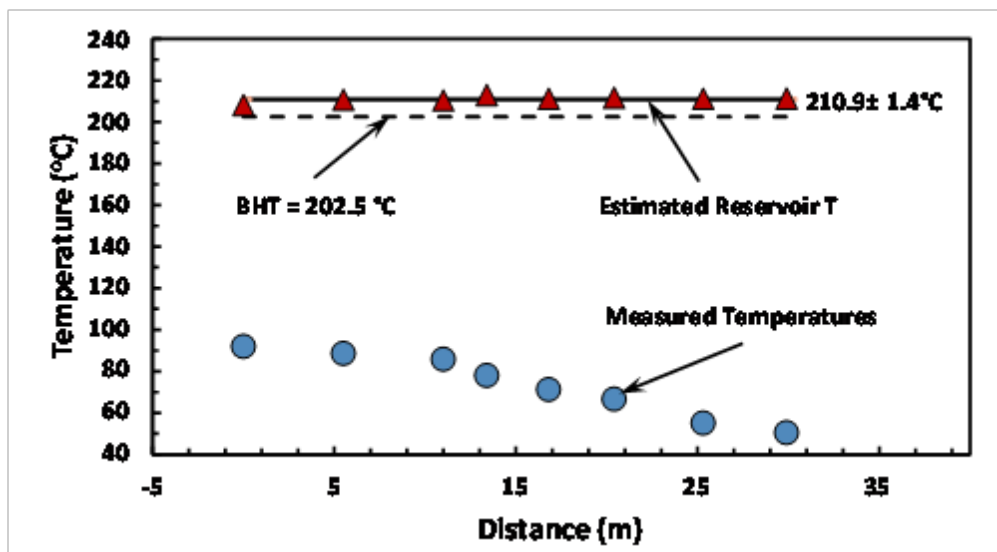


Figure 9. Measured sample temperatures (circles) and estimated reservoir temperatures (triangles) with distance along the overflow channel of Ojo Caliente Hot Spring. Solid line is the mean estimated reservoir temperature over all the samples. Dashed line in the measured bottom-hole temperature (BHT) from 157m in drill hole Y-2 located in the Lower Geyser Basin. Based on data from Ball et al. (1998)

## Boiling

Boiling of geothermal fluids results in the concentration of  $\text{SiO}_2(\text{aq})$  and other non-volatile constituents in the residual fluids and depletion of the fluid for volatiles such as  $\text{CO}_{2,\text{gas}}$  and  $\text{H}_2\text{S}_{\text{gas}}$ . Such alteration of the fluid chemistry by these processes complicates the interpretation of the chemical geothermometry and, if not considered, will increase uncertainty, and can lead to erroneous results. We illustrate the ability of RTEst to address such problems using data from geothermal wells in Iceland (Arnórsson et al., 1983a). This dataset includes downhole temperatures, steam fractions, liquid-fraction water compositions, and volatile concentrations from thermal waters that underwent boiling. The completeness of Arnórsson et al. (1983a) data allows for the reconstruction of the pre-boiling reservoir fluid. Because calculated hydrostatic pressures exceed the vapor saturation pressures, it is unlikely that boiling occurs in the reservoir, but rather it occurs in the well.

The two samples considered in these reconstruction calculations are the Hveragerdi Well 4 (sample 32) and the Námafjall Well 8 (sample 52). Measured downhole-temperatures for these wells are 180 and 246°C with steam fractions of 0.035 and 0.153, respectively. We summarize results of the reconstruction calculations and the RTEst optimizations for Hveragerdi Well 4 and Námafjall Well 8 in Figure 10. The first columns (blue) in the graphs are results of reconstructing the reservoir fluid using the measured temperature, steam fraction, and gas concentrations. Results for RTEst optimized temperature using the measured steam fraction and gas concentrations are given in the second column (orange). The third column (gray) results are for RTEst optimized temperature and GWB parameter reactTimes where the reactants are water and the measured volatile concentrations in the steam phase. The last column results (dark yellow) are also for optimization of temperature and reactTimes, but after the removed steam has been added back into the fluid. Reactants in the latter case are  $\text{CO}_{2,\text{gas}}$  (unit mass) and  $\text{H}_2\text{S}_{\text{gas}}$  whose mass is estimated from the aqueous  $\text{CO}_2/\text{H}_2\text{S}$  molal ratios and the ratios of the temperature-dependent Henry's Law constants (Appendix 2). Estimating the gas  $\text{CO}_2/\text{H}_2\text{S}$  mole ratios requires an estimate of the temperature (conventional  $\text{SiO}_2$  geothermometer), ionic strength (stoichiometric), and pH (estimated by optimization using  $\text{CO}_2$  only). The four cases presented in Tables 1 and 2 represent situations where complete information is available (column 1), information is fairly complete, but additional (conductive) heat loss may have occurred (column 2), gas concentrations are known but the steam quality is not known (column 3), and steam quality is known but gas concentration data is not available (column 4). For the Hveragerdi Well 4, minerals used in the loss function were chalcedony, calcite, analcime, and wairakite with Fe(III) concentrations calculated from goethite equilibrium (see Gunnlaugsson and Arnórsson, 1982). Quartz, albite-low, mordenite-K, laumontite, and forsterite were used for the Námafjall Well 8 loss function with Fe(III) calculated from hematite equilibrium (see Gunnlaugsson and Arnórsson, 1982) and calcite is allowed to react to maintain equilibrium.

Figure 10 shows that all four models give comparable results. Calculated temperatures are within 3°C of the measured values. Calculated steam quality for Hveragerdi and Námafjall wells are within 0.003 and 0.012 units of the measured values. Gas  $\text{CO}_2/\text{H}_2\text{S}$  mole ratios estimated in model 4 (0.061 and 0.487) are close to the measured values (0.074 and 0.525). The calculated pH with models 2, 3, and 4 are within 0.019 and 0.051 units of the pH calculated for the reconstructed reservoir fluid (for the Hveragerdi and Námafjall wells, respectively). Plots of  $n_{SD}$  versus temperature (Figure 11) show convergence of the saturation states for the minerals used in the loss functions and for other minerals potentially equilibrated with the reservoir fluids. The results are similar to those of Spycher et al. (2014) who obtained an average temperature of  $180 \pm 14^\circ\text{C}$  and an estimated steam fraction of  $\sim 0.06$  and by Reed and Spycher (1984) who obtained a temperature range of 175-185°C for Hveragerdi well and 205-245°C for the Námafjall well. The smaller uncertainties obtained in our study are likely the result of the specific minerals included in the loss function and the differences in the thermodynamic databases that were used. Traditional geothermometer estimates temperatures of 178.6, 168.6, 181.7°C for the Hveragerdi Well 4 for the

chalcedony, chalcedony with steam formation, and the Na/K geothermometers of Arnórsson et al. (1983b) and 244.1, 217.9, and 244.4°C for the quartz, quartz with steam formation, and Na/K geothermometers are in close agreement with the measured reservoir temperatures. These results demonstrate RTEst's ability to address boiling issues in hydrothermal systems.



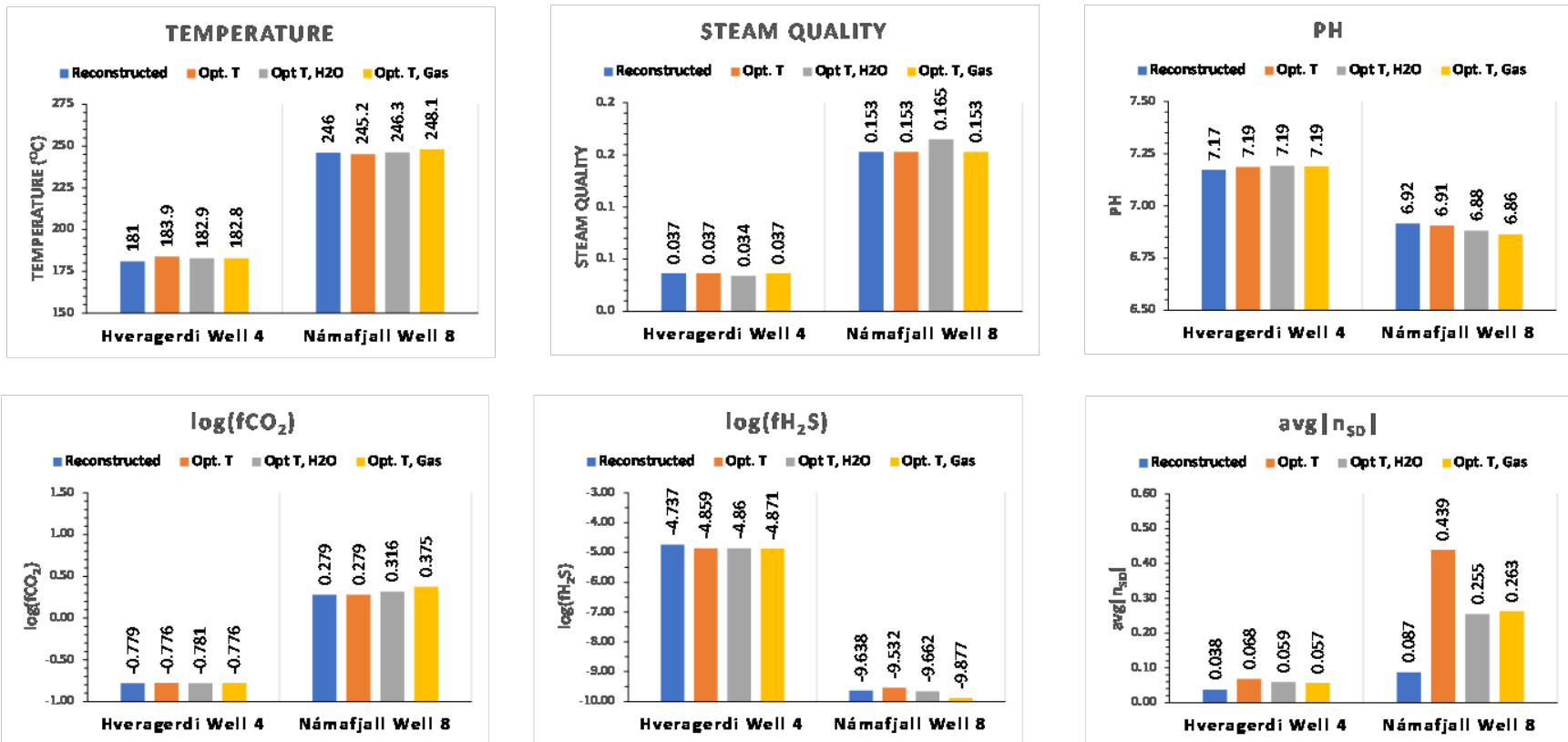


Figure 10. Results for the two Icelandic examples, Hveragerdi Well 4 and Námafjall Well 8. The first column (blue) is based on the measured values and does not use optimization. The three optimization models (columns 2, 3, and 4) are described in the text. Based on data from Arnórsson et al. (1983a).

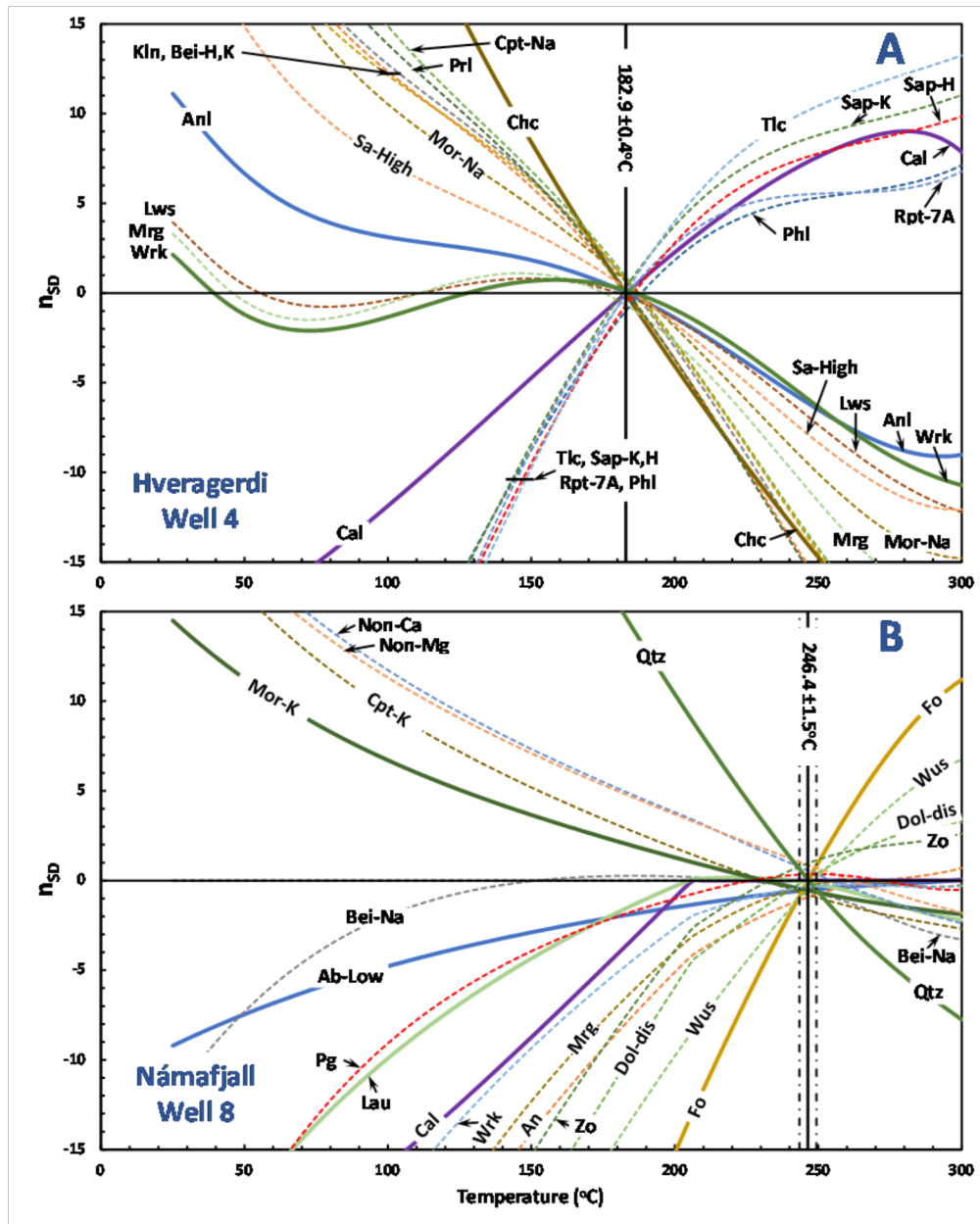


Figure 11. Plot of  $n_{SD}$  versus temperature for the Icelandic wells Hveragerdi Well 4 and Námafjall Well 8 for case 3 (optimize on temperature and  $\Delta H_2O$ , knowing the gas concentrations). Based on data from Arnórsson et al. (1983a). Mineral abbreviations are listed in Appendix 1.

## Missing and Unreliable Basis Species

Sometimes, chiefly with older data, basis species may be below the detection limit, missing, or unreliable. This may occur with Mg or Fe, but Al is particularly problematic because the saturation states for waters with respect to aluminosilicate minerals depend on  $\text{Al}^{3+}$  activity. Even with modern analytical methods, chemical processes and imperfect sampling procedures may result in concentrations that are not representative of the geothermal fluids. For example, Malkemus et al. (2021) observed Al concentrations in a thermal well decrease from 53 to  $4.0 \mu\text{g kg}^{-1}$  and Fe concentrations decrease from 316 to  $140 \mu\text{g kg}^{-1}$  as the well was purged. It is possible that the elevated concentrations result from the water interacting with corrosion product of well casing rather than rock-water interactions. It is also possible oxidation of Fe(II) with subsequent coprecipitation of Al with iron oxides biases Al concentrations toward lower values. Rather than discarding samples with no or questionable analyte measurements, we invoke some method of imputation.

One method of imputation is to calculate the analyte concentration based on the assumption of equilibrium with a mineral bearing that analyte (Pang and Reed, 1998). This condition is easily implemented in RTEst by swapping an analyte-bearing mineral thought to be controlling analyte concentrations for the basis species in the GWB React file. However, one limitation to this approach is choosing the analyte-bearing mineral that best represents the chemical conditions in the reservoir. An alternative method is to optimize the analyte concentration (Malkemus et al., 2021; Peiffer et al., 2014; Spycher et al., 2014). In RTEst, this method is implemented by adding a reactant (e.g.,  $\text{Al}(\text{OH})_{3(\text{aq})}$  for missing Al concentration) to the GWB React input file and optimizing on the reactTimes parameter.

To test this capability, we computed aluminum concentrations via optimization in RTEst and compared the results to measured Al concentrations for a sample of thermal water from a well (W3) at Breitenbush Hot Springs. The thermal water is equilibrated with calcite at the discharge temperature of  $71^\circ\text{C}$  and is believed not to have experienced significant  $\text{CO}_2$  outgassing (Malkemus et al., 2021). The mineral suite used in the loss function (chalcedony, laumontite, heulandite, celadonite, and epidote) is based on mineralogical identification in a 2,467-meter-deep drill hole (SUNEDCO 58-28) located  $\sim 3$  km southeast of the hot springs. Calcite is frequently reported in this drill hole, so the fluid is assumed to maintain equilibrium with calcite. In a separate application of RTEst, we fixed the Al concentration by using the measured value or imposing equilibrium with common aluminosilicate minerals. In addition, we estimated the Al concentration by optimization, as described above. The calculated reservoir temperatures fall within the narrow range of  $137.9 \pm 4.6$  to  $142.7 \pm 4.4^\circ\text{C}$  (Table 2) which is close to the maximum temperature ( $141^\circ\text{C}$ ) measured in the SUDEDCO 58-28 drill hole. The RTEst estimated temperature with the largest  $\text{avg}|n_{SD}|$  resulted from using the measured Al concentration. The RTEst estimated temperature with the smallest  $\text{avg}|n_{SD}|$  resulted from optimizing the Al concentration. The calculated reservoir temperature for this model ( $141.1 \pm 2.4^\circ\text{C}$ ) is nearly identical to the maximum (i.e., reservoir) temperature measured in the SUDEDCO 58-28 drill hole. The calculated Al concentration ( $9.0 \pm 1.3 \mu\text{g kg}^{-1}$ ) is lower than the measured value ( $15.8 \mu\text{g kg}^{-1}$ ) measured in the well. The optimized Al concentration is not significantly different from the average of the measured  $\text{Al}^{3+}$  concentrations at the site ( $8.3 \pm 4.6 \mu\text{g kg}^{-1}$ ), however, the range of optimized aluminum concentrations is less than the range of measured concentrations (Figure 9). Similarly, the temperatures based on the optimized Al concentrations are smaller. Standard deviations in the estimated temperatures based on optimized Al concentrations range from  $2.1$  to  $2.6^\circ\text{C}$  while those based on measured aluminum range from  $2.5$  to  $8.8^\circ\text{C}$ . These results demonstrate RTEst can estimate accurate geothermal reservoir temperatures from waters with missing Al (or other) measurements without the need to predefine an equilibrium aluminum bearing mineral.

Table 2. Calculated Al concentrations and reservoir temperatures for well W1 at the Breitenbush Hot Springs, Oregon. Based on data from Malkemus et al. (2021).

Method	Al ( $\mu\text{g kg}^{-1}$ )	$T_{\text{res}}$ ( $^{\circ}\text{C}$ )	avg n <sub>SD</sub>
Measured	15.8	142.2 $\pm$ 5.1	1.136
Albite	14.6	137.9 $\pm$ 4.6	1.134
Muscovite	5.8	142.7 $\pm$ 4.4	0.981
Kaolinite	11.4	140.1 $\pm$ 2.8	0.565
Smectite-High-Fe-Mg	11.0	141.9 $\pm$ 2.5	0.541
K-Feldspar	8.0	142.7 $\pm$ 2.1	0.528
Smectite-Low-Fe-Mg	7.3	141.0 $\pm$ 2.7	0.524
Illite	9.9	140.7 $\pm$ 2.2	0.427
Optimized	9.0 $\pm$ 1.3	141.1 $\pm$ 2.4	0.398
<b>Meas. Site Avg.</b>	<b>8.3 <math>\pm</math> 4.6</b>	<b>141</b>	

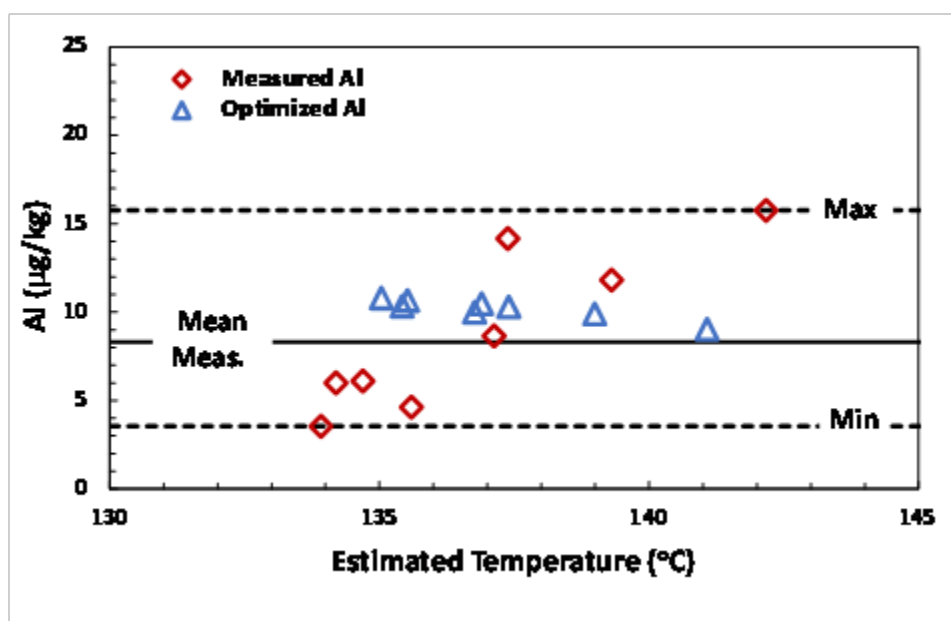


Figure 12. Measured and calculated aluminum concentrations versus temperature for thermal springs and wells at Breitenbush Hot Springs, Oregon, USA. Based on data from Malkemus et al. (2021).

## Mixing

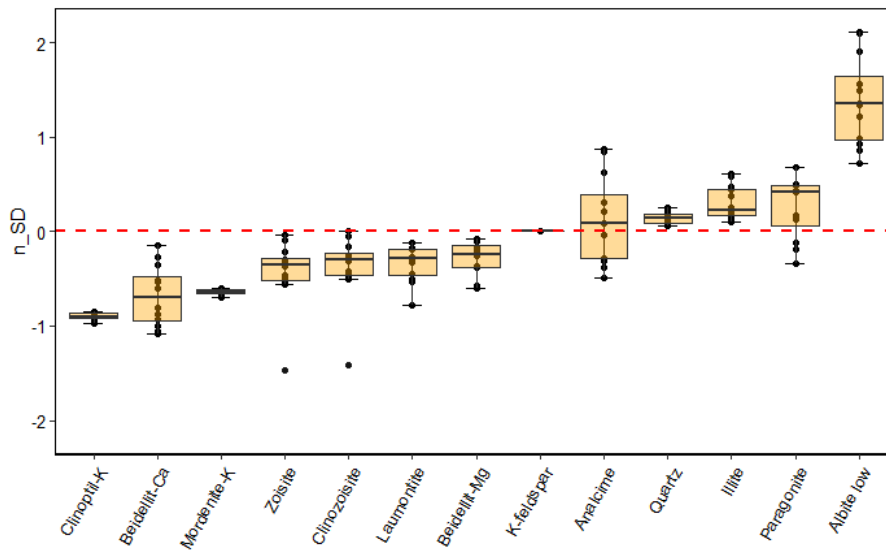
It is common for thermal waters to mix with near-surface non-thermal waters. For example, most thermal waters in Yellowstone National Park are considered mixed (Parry and Bowman, 1990). RTEst can estimate the mixing fraction using the GWB React reactTimes parameter. To illustrate this capability, we used data from thermal springs in the Boundary Creek area (Upper, Middle, and Lower Boundary Creek and Silver Scarf springs) of southwestern YNP along the border between Wyoming and Idaho, USA (Parry and Bowman, 1990; Parry et al., 1981). The Cold Spring, located in the Upper Boundary Creek area is presumed to represent the non-thermal water diluting the thermal water to give the various

temperature thermal springs. The temperature of Cold Springs is 13.8°C with Na<sup>+</sup>, Cl<sup>-</sup>, and SiO<sub>2</sub>(aq) concentrations of 6, 1, and 32 mg/L, respectively. In contrast, the hot springs have temperatures ranging from 54 to 89°C, Na<sup>+</sup> from 84 to 185 mg/L, Cl<sup>-</sup> 38 to 95 mg/L, and SiO<sub>2</sub>(aq) from 159 to 230 mg/L

The minerals used in the loss function (quartz, illite, mordenite-K, analcime, laumontite) have been identified in boreholes within YNP (Bargar and Beeson, 1981, 1984; Honda and Muffler, 1970; Keith and Muffler, 1978; Keith et al., 1978). Aluminum concentrations were calculated assuming equilibrium with K-feldspar which is reasonable given the identification of adularia in several boreholes. In addition, we assume the rate of reaction of calcite is sufficiently rapid to maintain equilibrium with the reservoir fluid. This presumption implies that Ca and TIC concentrations in the reservoir are less than those measured in the discharge. Illite was chosen because 1) it has a narrower compositional range compared to the more frequently reported montmorillonite and mixed-layered montmorillonite-illite interlayered clays, 2) it occurs more frequently at higher temperatures/greater depths, and 3) the mixed-layered montmorillonite-illite clays are dominated by the illitic fraction (Bargar and Beeson, 1981, 1984). Temperature and mixing fraction were calculated using RTEst optimization. If the optimized reactTimes parameter for a spring was less than 1.96 standard deviations from zero (i.e., less than the 95% confidence level), the sample was re-run assuming that no mixing had occurred (i.e., reactTimes was zero) with temperature being the only optimized parameter.

The minerals used in the loss function and several other minerals are within one standard deviation from saturation (Figure 13). A plot of  $n_{SD}$  versus temperature (Figure 14) shows convergence of the saturation indexes for these minerals. Besides the minerals used in the loss function, clinoptilolite-K, beidellite (-Ca, -Mg), zoisite and paragonite saturation indices approach zero at the optimized temperature. Clinoptilolite is common in several boreholes so its near-zero SI at the optimized temperature should be expected. Beidellite is not specifically reported, however it can be considered representative of the more Al-rich tetrahedral component of the observed montmorillonite and montmorillonite-illite interlayered smectites observed in the boreholes. Similarly, though it is not observed, paragonite represents the Na-rich component of the structurally similar illite. A plot of SiO<sub>2</sub>(aq) versus temperature (Figure 15) shows the estimated reservoir temperatures for individual springs clustered over a small temperature range, with an average of 205.1 ± 2.5°C. The model suggests that conductive cooling of the reservoir fluid followed by mixing with waters similar to Cold Spring is a reasonable hypothesis. In contrast, the application of quartz, quartz with steam formation, and the Na-K-Ca geothermometers give a wide range of reservoir temperatures (143-189, 138-176, and 135-161°C, respectively) (Parry and Bowman, 1990; Parry et al., 1981) whose maximum values are less than what is estimated with the RTEst program. Even after correcting for dilution, the average traditional geothermometer estimates across the samples are 190.2 ± 3.6, 179.1 ± 2.7, and 114.5 ± 19.5°C for the quartz, quartz with steam formation, and Na/K given by Arnórsson et al. (1983b) yield different results and all are lower than the RTEst predicted reservoir temperature.

Figure 13. Box and whiskers diagram of the  $n_{SD}$  for the minerals within 1.0 standard deviations from saturation. Boundary Creek area, Yellowstone National Park.



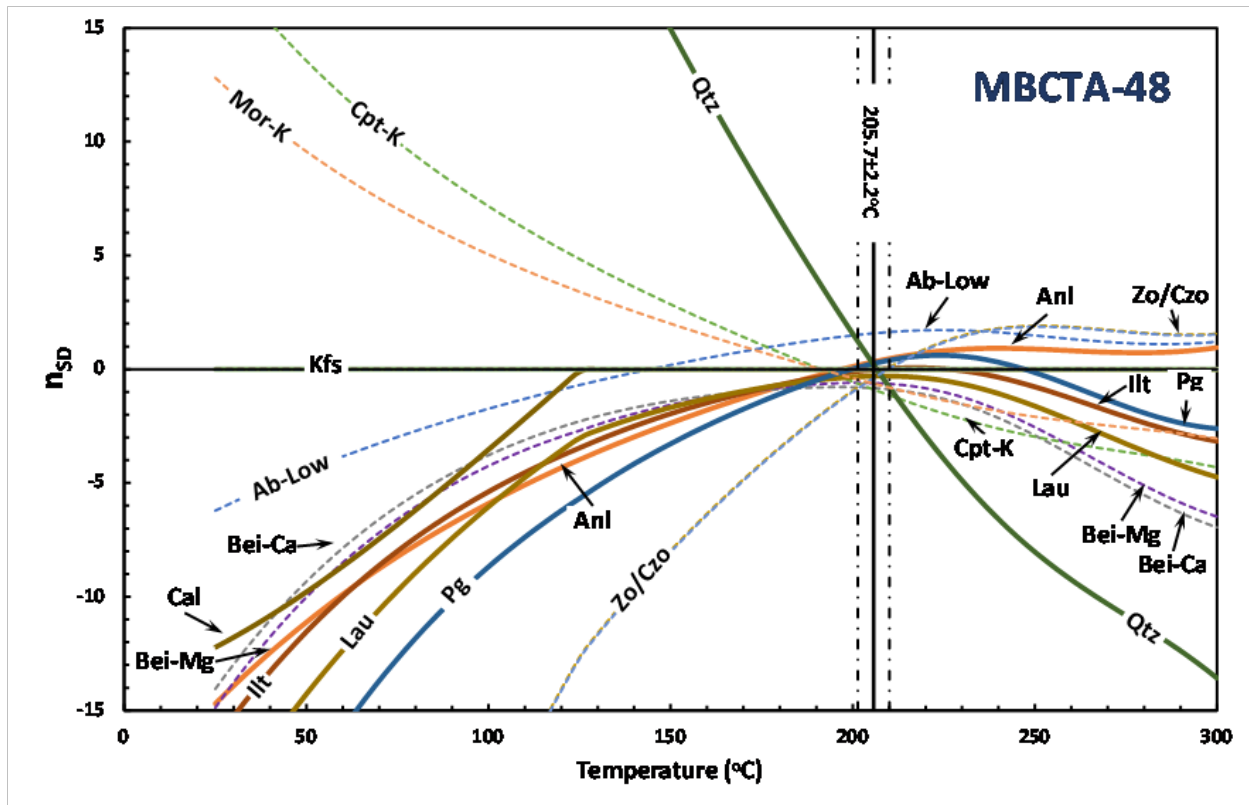


Figure 14. Plot of  $n_{SD}$  versus temperature for sample MBCTA-48 from the Middle Boundary Creek area, YNP. Optimized fraction of thermal water is  $0.82 \pm 0.02$  is used at all temperatures in the plot. Mineral abbreviations are listed in Appendix 1.

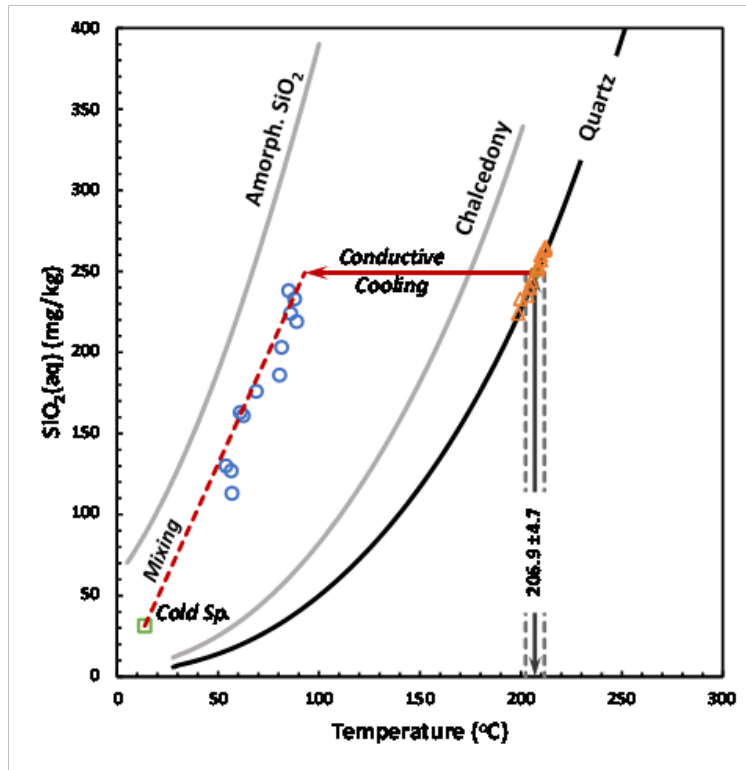


Figure 15.  $\text{SiO}_2(\text{aq})$  concentrations versus temperature for measured values (blue circles) and calculated values in the reservoir (orange triangles). The dashed red line is the mixing curve based on the mixing fractions from the optimization. The water is assumed to have cooled to 93°C, the boiling temperature of pure water at the approximate elevation of the springs (1980 – 2280 m).

The mixing fractions calculated using RTEst are based on saturation states for minerals in the loss function and a known end-member composition (often the non-thermal water). Mixing fractions are more commonly calculated using conservative analytes, such as  $\text{Cl}^-$  with known end members. Comparing the mixing fractions for the Boundary Creek thermal area calculated via RTEst optimization with those calculated from  $\text{Cl}^-$  and  $\text{Na}^+$  (Figure 16) shows high correlation ( $r = 0.972$  and  $r = 0.931$ , respectively) between the two methods. These results demonstrate that RTEst can effectively estimate reservoir temperature for thermal features that are the product of the mixing of thermal waters with cold near-surface waters.

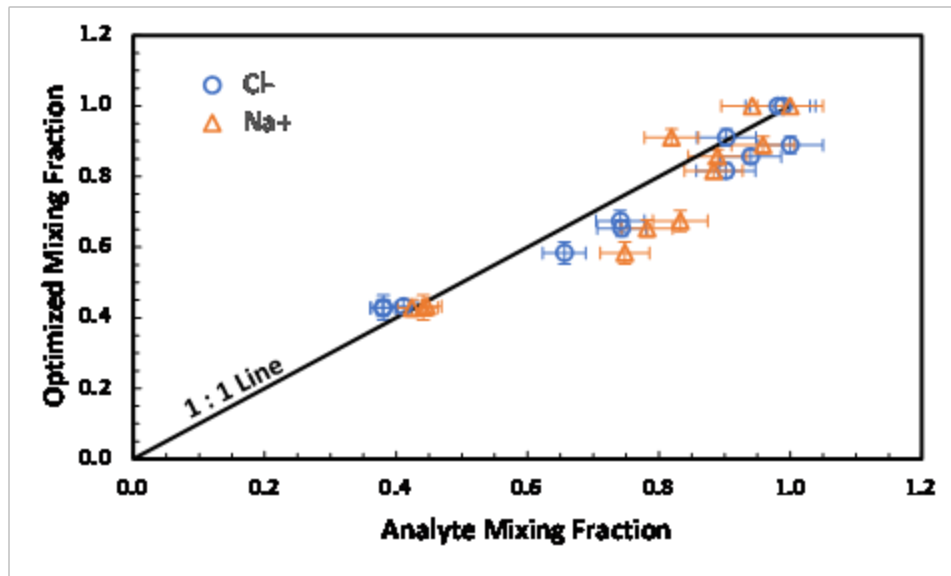


Figure 16. Mixing fraction calculated from optimization using RTEst versus mixing fraction based on analyte concentration. The mixing fraction is the fraction of thermal water in the mixture.

### Effect of Weighting Factors

All the examples examined thus far use the inverse of variance of weighting option. To illustrate the advantage of this method, we have rerun the first example (Breitenbush W1 sample assuming calcite equilibrium) with unit weights and normalization (Table 3). Using inverse of variance, the estimated reservoir temperature for this sample is  $139.5 \pm 2.6^\circ\text{C}$  with an  $\text{avg}|n_{SD}|$  for the minerals in the loss function (chalcedony, celadonite, laumontite, heulandite, epidote) of 0.71. Solving the same problem using unit weights yields a reservoir temperature of  $143.9 \pm 2.4^\circ\text{C}$ . The ostensibly lower uncertainty in the temperature estimate may lead one to suspect that this latter estimate with unit weighting is a better estimate of the reservoir temperature, however, this variance is likely underestimated because of heteroscedasticity. The average  $\text{avg}|n_{SD}|$  for the unit weight case (0.85) is larger than the  $\text{avg}|n_{SD}|$  for the inverse of variance method. Further, the  $n_{SD}$  for chalcedony is 2.1 indicating a probability  $< 0.05$  that this mineral is not equilibrated with the fluid given the associated analytical uncertainty and thermodynamic database. The normalization method gives results similar to the case of unit weights (Table 3). While the difference in temperature between unit and inverse of variance weighting is small in this example, under some conditions, it can be more pronounced.

Consider the same problem but include only chalcedony, celadonite, and laumontite in the loss function (Table 3). For the inverse of variance weighting, the estimated reservoir temperature ( $138.9 \pm 4.1^\circ\text{C}$ ) is nearly identical to what was obtained using the original five minerals in the loss function. The uncertainty in the temperature and the  $\text{avg}|n_{SD}|$  (0.99) are slightly larger, as expected with the inclusion of laumontite. In contrast, the unit weighting method gives a significantly higher temperature ( $152.1 \pm 3.1^\circ\text{C}$ ) and an  $\text{avg}|n_{SD}|$  (1.6) that is nearly double the value obtained using the original five minerals in the loss function. The  $n_{SD}$  for chalcedony is now 4.4. The measured reservoir temperature at Breitenbush hot springs ( $141^\circ\text{C}$ ) is within 0.51 standard deviations from the estimate based on inverse of variance weighting, while it is 3.6 standard deviations from the estimate based on unit weighting. Again, the results for the normalization method are more similar to those obtained using unit weighting (Table 3). The overestimate of the reservoir temperature using the unit weighting approach with the small uncertainty is a consequence of not accounting for the inherent heteroscedasticity in the multicomponent geothermometry problem and should not be interpreted as more representative estimate of reservoir temperature. The

example shows the improved reservoir estimates using inverse of variance over the unit weighting and normalization methods.

Table 3. Comparison of different weighting methods for Breitenbush sample W01. Based on data from Malkemus et al. (2021). All  $n_{SD}$  based on inverse of variance for consistent comparison.

<b>Weighting</b>	<b>Minerals in Loss Function</b>	<b>Temperature (°C)</b>	<b>avg <math>n_{SD}</math> </b>	<b><math>n_{SD}</math> (Chc)</b>
Inverse Variance	Chc-Cel-Lau-Hul-Ep	139.5 ±2.6	0.71	0.90
Normalization	Chc-Cel-Lau-Hul-Ep	144.0 ±2.6	0.85	2.14
Unit Weight	Chc-Cel-Lau-Hul-Ep	143.9 ±2.4	0.85	2.10
Inverse Variance	Chc-Cel-Lau	138.9 ±4.1	0.99	0.71
Normalization	Chc-Cel-Lau	149.7 ±5.0	1.43	3.71
Unit Weight	Chc-Cel-Lau	152.1 ±3.1	1.64	4.36

### RTEst Application

To date, we have applied RTEst in several geothermometry investigations. A study of the deep geothermal waters of the Eastern Snake River Plain of Idaho (Neupane et al., 2014) estimated reservoir temperatures up to  $154 \pm 5^\circ\text{C}$  using the normalization weights. This study was later expanded with collection and analysis of additional water samples from several hot springs and thermal wells around the Eastern Snake River Plain (e.g., Cannon et al., 2014; Mattson et al., 2015; Neupane, Ghanashyam et al., 2016a; Neupane, Ghanashyam et al., 2016b), representing geothermal reservoirs hosted in diverse rock types such as basalt, rhyolite, granite, and carbonate. These studies used RTEst as the primary tool to estimate reservoir temperatures and helped identify several geothermal prospects within and along the margins of the Eastern Snake River Plain with reservoir temperatures ranging from 140 to  $200^\circ\text{C}$ . Subsequently, RTEst reservoir temperatures calculated for water samples from numerous hot springs and thermal wells were used as an input layer in the geothermal play fairway analysis of the Snake River Plain (Shervais et al., 2017; Shervais et al., 2018; Shervais et al., 2015; Shervais et al., 2020).

In another study that encompassed thermal features in southeastern Idaho (Neupane, G. et al., 2016), RTEst was used to identify promising thermal features in the Preston area. A follow-up study of that geothermal system (Wood et al., 2015) suggested that the thermal waters are equilibrated with illite, calcite, paragonite, mordenite-K, and a  $\text{SiO}_2$  polymorph (quartz/chalcedony). Neupane et al. (2015) used RTEst to model fluids from four geothermal power plants (Raft River, Idaho; Neal Hot Springs, Oregon, Roosevelt Hot Springs, Utah; and Steamboat Springs, Nevada) in the western United States. In general, they found good agreement between the temperatures of the producing reservoir estimated from the composition of shallow thermal features with RTEst and the measured bottom-hole temperatures suggesting that RTEst can predict temperatures prior to geothermal energy development. Mattson et al. (2015) assessed the validity of RTEst as a geothermometry tool by applying it to water samples reacted with rock at known temperatures. Batch-type water-rock experiments involved metamorphosed quartz monzonite and synthetic Raft River geothermal water reacted at 150 and  $200^\circ\text{C}$  for more than 10 months. RTEst estimated temperatures for multiple water samples collected at various times were within  $\pm 5^\circ\text{C}$  of experimental temperature. Malkemus et al. (2021) provide revised temperatures estimates of the reservoir associated with the Breitenbush Hot springs, Oregon that agree with the maximum temperature measured in a 2,457-meter-deep borehole near the springs.

## Summary and Conclusions

RTEst can accurately predict reservoir temperatures even when physical and chemical process alter the geochemistry of the fluids as they ascend toward the surface. We illustrate this capability in examples which include i) alteration of the chemical composition of the fluid by mineral reaction, ii)  $\text{CO}_{2,\text{gas}}$  loss by degassing, iii) boiling of fluids during ascension, and iv) mixing of thermal and non-thermal waters. In addition, RTEst can handle data sets with missing or unreliable data such as Al, Fe, or Mg concentrations.

RTEst often better predicts reservoir temperatures than traditional geothermometers. Many of the RTEst estimates were closer to the measured temperatures than the quartz geothermometer. This result is most likely the consequence of the choice of quartz geothermometer (Arnórsson et al., 1983b) as temperatures from different quartz geothermometers vary from  $\sim 15^\circ\text{C}$  at  $200 \text{ mg kg}^{-1}$  to nearly  $30^\circ\text{C}$  at  $600 \text{ mg kg}^{-1}$  (Cioni and Marini, 2020). In addition, quartz solubility in seawater is greater than it is in pure water (Cioni and Marini, 2020) which can overestimate the reservoir temperature by as much as  $10^\circ\text{C}$  at temperatures ca.  $300^\circ\text{C}$ . While traditional geothermometry does not account for such an effect, the GWB React module used in RTEst corrects for this outcome via its activity coefficient model for electrically neutral, nonpolar species such as  $\text{SiO}_{2,\text{aq}}$  (Bethke, 2008). Uncertainty in the estimated reservoir temperatures across the various geothermometers is much greater than the uncertainty obtained using RTEst. This variation is driven mainly by our choice of Na/K geothermometer which often yields quite different results than the quartz geothermometers. This difference is primarily the result of large variation in Na/K geothermometers (as much as  $50^\circ\text{C}$  at the same Na/K) many of which are empirically derived and may not apply to the specific system being studied (Cioni and Marini, 2020).

RTEst represents a major advancement in geothermometry over the original multicomponent approach of Reed and Spycher (1984) because it circumvents the graphical method of identifying the intersection point of saturation indexes by using of the optimization approach tools in PEST<sup>®</sup> (Doherty, 2015, 2018a, b). This approach also allows for optimization of multiple parameters besides temperature. The multicomponent optimization approach makes RTEst similar to the GeoT program (Spycher et al., 2014). Indeed, a comparison of the two models using the data from the Breitenbush Hot Springs, Oregon, yielded nearly identical reservoir temperatures (Malkemus et al., 2017). A key advantage of RTEst is the use of the inverse of variance weighting approach that appears to alleviate issues associated with the inherent heteroscedasticity of multicomponent geothermometry better than the unit weighting or normalization methods. Also, RTEst is based on The Geochemist's Workbench<sup>®</sup> and PEST<sup>®</sup>, well-known software tools that will allow rapid adaption by users. Another advantage of RTEst is the mineral selection tool that can help users select the minerals by filters based on lithology, pH, and temperature range. While this approach is useful, better methods for mineral identification are under development and could be incorporated into RTEst. Another key area of development is improved data management. Geothermometry generates large volumes of output from multiple springs and wells that needs to more easily searched, filtered, and visualized.

Beyond using geothermometry for calculating reservoir conditions for a single spring or well or a group of samples equilibrated with the same portion of the reservoir, geothermometry can be used to gain insights into the underlying structure of a geothermal system. Malkemus et al. (2021) generated a map of geothermometric temperatures that shows potential alignment with underlying fault systems. They also showed that reconstituted discharge waters fall into two groups of samples at different temperatures for the transition from closed to open system  $\text{CO}_2$  which has implications to residence times in fractures.

Such information could be invaluable to the development and testing of thermal transport models of geothermal systems.

The emphasis in geothermometry has been on determining the temperature of the underlying reservoir. However, multicomponent geothermometry also provides information about the geochemical conditions within the reservoir, namely pH,  $f\text{CO}_2$ , Ca concentrations. Such information is essential in estimating scale formation. While multicomponent geothermometry has been applied to primarily natural hydrothermal systems, many of the concepts discussed here also apply to other thermal systems such as Enhanced Geothermal Systems (EGS) and Reservoir Thermal Energy Storage (RTES) systems. RTES can be a valuable tool for assessing these less conventional types of geothermal systems in addition to more conventional hydrothermal systems.

## Appendix 1: Mineral Abbreviations.

Abbreviations for selected minerals from the modified thermo.tdat database. Abbreviations are based primarily on Whitney and Evans (2010).

<b>Abbreviation</b>	<b>Mineral</b>	<b>Abbreviation</b>	<b>Mineral</b>
<b>Ab-Low</b>	<b>Albite-Low</b>	<b>Mor-K</b>	<b>Mordenite-K</b>
<b>Anl</b>	<b>Analcime</b>	<b>Mor-Na</b>	<b>Mordenite-Na</b>
<b>Bei-Ca</b>	<b>Beidellite-Ca</b>	<b>Mrg</b>	<b>Margarite</b>
<b>Bei-H</b>	<b>Beidellite-H</b>	<b>Non-Ca</b>	<b>Nontronite-Ca</b>
<b>Bei-K</b>	<b>Beidellite-K</b>	<b>Non-K</b>	<b>Nontronite-K</b>
<b>Bei-Mg</b>	<b>Beidellite-Mg</b>	<b>Non-Mg</b>	<b>Nontronite-Mg</b>
<b>Bei-Na</b>	<b>Beidellite-Na</b>	<b>Non-Na</b>	<b>Nontronite-Na</b>
<b>Cal</b>	<b>Calcite</b>	<b>Pg</b>	<b>Paragonite</b>
<b>Cel</b>	<b>Celadonite</b>	<b>Ptl</b>	<b>Petalite</b>
<b>Chc</b>	<b>Chalcedony</b>	<b>Ph</b>	<b>Phengite</b>
<b>Cpt-Ca</b>	<b>Clinochlore-Ca</b>	<b>Phl</b>	<b>Phlogopite</b>
<b>Cpt-K</b>	<b>Clinochlore-K</b>	<b>Prl</b>	<b>Pyrophyllite</b>
<b>Cpt-Na</b>	<b>Clinochlore-Na</b>	<b>Qtz</b>	<b>Quartz</b>
<b>Czo</b>	<b>Clinozoisite</b>	<b>Rip-7A</b>	<b>Rapidite-7A</b>
<b>Dol-dis</b>	<b>Dolomite-dis</b>	<b>Rip-14A</b>	<b>Rapidite-14A</b>
<b>Ep</b>	<b>Epidote</b>	<b>Sa-High</b>	<b>Saralite-High</b>
<b>FeO(c)</b>	<b>FeO(c)</b>	<b>Sap-H</b>	<b>Saponite-H</b>
<b>Fo</b>	<b>Forsterite</b>	<b>Sap-K</b>	<b>Saponite-K</b>
<b>Fs</b>	<b>Ferrosilite</b>	<b>Sd</b>	<b>Siderite</b>
<b>Gth</b>	<b>Goethite</b>	<b>Sme-High</b>	<b>Smectite-high-Fe-Mg</b>
<b>Hul</b>	<b>Heulandite</b>	<b>Sme-Low</b>	<b>Smectite-low-Fe-Mg</b>
<b>Ill</b>	<b>Illite</b>	<b>Str</b>	<b>Strunzite</b>
<b>Kln</b>	<b>Kaolinite</b>	<b>Tlc</b>	<b>Talc</b>
<b>Kfs</b>	<b>K-feldspar</b>	<b>Wik</b>	<b>Wairakite</b>
<b>Lau</b>	<b>Laumontite</b>	<b>Wus</b>	<b>Wustite</b>
<b>Lws</b>	<b>Lawsontite</b>	<b>Zo</b>	<b>Zoisite</b>
<b>Max-Mc</b>	<b>Maximum Microcline</b>		

## Appendix 2: H<sub>2</sub>S/ CO<sub>2</sub> Gas Ratios in Steam

Geothermometry calculation depend on the pH of the fluid which is often calculated after reconstructing the water composition by adding back lost volatiles. In our applications of RTEst, we have focused on CO<sub>2</sub> since in most cases it is the volatile with the most impact on the pH of the reconstructed fluid. However, other gases can also impact the fluid pH and should be considered. In its current formulation, RTEst does not treat additional gases directly, however, they can be added via the GWB reactTimes parameter (along with CO<sub>2</sub>) if the ratio of the gases is known. We show how to estimate this ratio by focusing on H<sub>2</sub>S, although, the same approach can be used for other gases.

For an isoenthalpic system where the pressure is reduced and the system remains closed with respect to mass, a two-phase system forms as water and volatiles such as CO<sub>2</sub> partition into the vapor phase. A mass balance for CO<sub>2</sub> requires that

(6)

where  $C_{C,R}$  and  $C_{C,1}$  are the total concentrations of CO<sub>2</sub> in the reservoir before volatilization and the measured CO<sub>2</sub> in the liquid phase after volatilization, and  $x_v$ ,  $f(\text{CO}_2)$ ,  $\rho_v$ ,  $T$ , and  $R$  are the fraction of water in the steam phase, the fugacity of CO<sub>2</sub>, the density of the vapor, temperature (K), and the gas constant. The fugacity coefficient of CO<sub>2,gas</sub> ( $\gamma(\text{CO}_2)$ ), is assumed to be equal to unity. The fugacity in the gas phase is related to CO<sub>2</sub>(aq) via Henry's constant. Using HCO<sub>3</sub><sup>-</sup> as the basis species for the inorganic carbon species, we can write  $f(\text{CO}_2)$  as

(7)

where the square brackets denote the activities of the species. Substituting Eq. (7) into Eq. (6) we have

(8)

The first term on the RHS of Eq. (8) accounts for the concentration of solutes as a result of liquid water being converted to steam and is included by adding a reaction term to the \*.rea file that is 1 kg H<sub>2</sub>O and a reactTimes values equal to  $x_v$ . The second term of the RHS are the volatiles that are in the steam phase that need to be added back into the liquid to reconstruct the reservoir fluid. This term is also added back as a reaction term as a mass per mass of steam. We concentrate on this second term which we designate at  $\Delta C$ :

(9)

The [HCO<sub>3</sub><sup>-</sup>] can be written in terms of the  $C_{C,1}$  as

(10)

)

where the  $\gamma_i$  denote the activity coefficients of the  $i$ th species. Writing the terms on the right-hand side with the activity of the common basis species HCO<sub>3</sub><sup>-</sup> and rearranging, we obtain

(11)

)

Substituting Eq. (11) into Eq. (9) yields

(12)

The analogous equation for sulfide is

(13)

Dividing Eq. (13) by Eq. (12) yields

(14)

or

(15)

Thus, if we have an estimate of the pH, ionic strength, and temperature, we can estimate the sulfide/CO<sub>2</sub> ratio in the steam phase and use this ratio in the optimization using RTEst. Similar ratios can also be determined for other gases. We have set up a spreadsheet to make this estimate. This sheet reasonably replicates the values in Arnórsson et al. (1983a).

## References

- Arnórsson, S., Gunnlaugsson, E., Svavarsson, H., 1983a. The chemistry of geothermal waters in Iceland. II. Mineral equilibria and independent variables controlling water compositions. *Geochimica et Cosmochimica Acta* 47(3), 547-566.
- Arnórsson, S., Gunnlaugsson, E., Svavarsson, H., 1983b. The chemistry of geothermal waters in Iceland. III. Chemical geothermometry in geothermal investigations. *Geochimica et Cosmochimica Acta* 47(3), 567-577.
- Ball, J.W., McCleskey, R.B., Nordstrom, D.K., Holloway, J.M., Verplanck, P.L., Sturtevant, S.A., 2002. Water-chemistry data for selected springs, geysers, and streams in Yellowstone National Park, Wyoming, 1999-2000, Open-File Report. Reston, VA.
- Ball, J.W., McMleskey, R.B., Nordstrom, D.K., 2010. Water-chemistry data for selected springs, geysers, and streams in Yellowstone National Park, Wyoming, 2006-2008, Open-File Report. Reston, VA.
- Ball, J.W., Nordstrom, D.K., Cunningham, K.M., Schoonen, M.A., Xu, Y., DeMonge, J.M., 1998. Water-chemistry and on-site sulfur-speciation data for selected springs in Yellowstone National Park, Wyoming, 1994-1995, Open-File Report. Reston VA.
- Bargar, K.E., Beeson, M.H., 1981. Hydrothermal alteration in research drill hole Y-2, Lower Geyser Basin, Yellowstone National Park, Wyoming. *American Mineralogist* 66(5-6), 473-490.
- Bargar, K.E., Beeson, M.H., 1984. Hydrothermal alteration in research drill hole Y-6, Upper Firehole River, Yellowstone National Park, Wyoming, Professional Paper, - ed.
- Bargar, K.E., Oscarson, R.L., 1997. Zeolites and selected other hydrothermal minerals in the Cascade Mountains of northern Oregon, Open-File Report, - ed.
- Barger, K.E., 1994. Hydrothermal alteration in the SUNEDCO 58-28 geothermal drill hole near Breitenbush Hot Springs, Oregon. *Oregon Geology* 56(4), 75-87.
- Bethke, C.M., 2008. *Geochemical and Biogeochemical Reaction Modeling*, 2nd ed. Cambridge University Press, New York, New York, USA.
- Bethke, C.M., Yeakel, S., 2014a. *The Geochemist's Workbench Release 10 Reaction Modelling Guide. Aqueous Solutions*, LLC, Champaign, IL, p. 106.
- Bethke, C.M., Yeakel, S., 2014b. *The Geochemist's Workbench Release 10 Reference Manual. Aqueous Solutions*, LLC, Champaign, IL, p. 462.
- Browne, P.R.L., 1978. Hydrothermal Alteration in Active Geothermal Fields. *Annual Review of Earth and Planetary Sciences* 6(1), 229-248.

- Cannon, C., Wood, T., Neupane, G., McLing, T., Mattson, E., Dobson, P., Conrad, M., 2014. Geochemistry sampling for traditional and multicomponent equilibrium geothermometry in southeast Idaho. *GRC Transactions* 38, 425-431.
- Cioni, R., Marini, L., 2020. *A Thermodynamic Approach to Water Geothermometry*. Springer Geochemistry.
- Cooper, D.C., Palmer, C.D., Smith, R.W., McLing, T., 2013. Multicomponent equilibrium models for testing geothermometry approaches, *Proceeding of the Thrity-Eighth Workshop on Geothermal Reservoir Engineering*. Stanford University, Stanford, California, February 11-13, 2013 SGP-TR-204
- D'Amore, F., Fancelli, R., Caboi, R., 1987. Observations on the application of chemical geothermometers to some hydrothermal systems in Sardinia. *Geothermics* 16(3), 271-282.
- Doherty, J., 2015. *Calibration and Uncertainty Analysis for Complex Environmental Models*. Watermark Numerical Computing, Brisbane, Australia.
- Doherty, J., 2018a. *PEST, Model-Independent Parameter Estimation User Manual Part I: Pest, SENSAN and Global Optimisers*, 7th ed. Watermark Numerical Computing, Brisbane, Australia.
- Doherty, J., 2018b. *PEST, Model-Independent Parameter Estimation User Manual Part II: PEST Utility Support Software* 7th ed. Watermark Numerical Computing, Brisbane, Australia.
- Fouillac, C., Michard, G., 1981. Sodium/lithium ratio in water applied to geothermometry of geothermal reservoirs. *Geothermics* 10(1), 55-70.
- Fournier, R.O., 1977. Chemical geothermometers and mixing models for geothermal systems. *Geothermics* 5(1-4), 41-50.
- Fournier, R.O., Potter, R.W., 1979. Magnesium correction to the Na-K-Ca chemical geothermometer. *Geochimica et Cosmochimica Acta* 43(9), 1543-1550.
- Fournier, R.O., Rowe, J.J., 1966. Estimation of underground temperatures from the silica content of water from hot springs and wet-steam wells. *American Journal of Science* 264(9), 685-697.
- Fournier, R.O., Sorey, M.L., Mariner, R.H., Truesdell, A.H., 1979. Chemical and isotopic prediction of aquifer temperatures in the geothermal system at Long Valley, California. *Journal of Volcanology and Geothermal Research* 5(1-2), 17-34.
- Fournier, R.O., Truesdell, A.H., 1973. An empirical Na-K-Ca geothermometer for natural waters. *Geochimica et Cosmochimica Acta* 37(5), 1255-1275.
- Fournier, R.O., White, D.E., Truesdell, A.H., 1974. Geochemical indicators of subsurface temperature; Part I, Basic assumptions. *Journal of Research, U.S. Geol. Survey* 2(3), 259-262.
- Giggenbach, W.F., 1988. Geothermal solute equilibria. Derivation of Na-K-Mg-Ca geothermometers. *Geochimica et Cosmochimica Acta* 52(12), 2749-2765.
- Glacier Partners, 2009. *Geothermal Economics 101, Economics of a 35 MW Binary Cycle Geothermal Plant*. p. 46.
- Greene, W.H., 2018. *Econometric Analysis*, Eighth ed. Pearson, New York, NY.
- Gunnlaugsson, E., Arnórsson, S., 1982. The chemistry of iron in geothermal systems in Iceland. *Journal of Volcanology and Geothermal Research* 14(3), 281-299.
- Honda, S., Muffler, L.J.P., 1970. Hydrothermal alteration in core from research drill hole Y-1, upper geyser basin, Yellowstone National Park, Wyoming. *American Mineralogist* 55(9-10), 1714-1737.
- Hull, C.D., Reed, M.H., Fisher, K., 1987. Chemical Geothermometry and Numerical Unmixing of the Diluted Geothermal Waters of the San Bernardino Valley Region of Southern California. *Geothermal Resources Council Transactions* 11, 165-184.
- Keith, T.E.C., Muffler, L.J.P., 1978. Minerals produced during cooling and hydrothermal alteration of ash flow tuff from Yellowstone drill hole Y-5. *Journal of Volcanology and Geothermal Research* 3(3-4), 373-402.
- Keith, T.E.C., White, D.E., Beeson, M.H., 1978. Hydrothermal alteration and self-sealing in Y-7 and Y-8 drill holes in northern part of upper Geyser Basin, Yellowstone National Park, Wyoming, *Professional Paper 1054A*, - ed.
- Malkemus, D., Perkins, R.B., Palmer, C.D., 2017. Geothermometry of Breitenbush Hot Spring, Oregon, USA, *Proceedings 5th Indonesia International Geothermal Convention and Exhibit (IIGCE)*.

- Jakarta, Indonesia.
- Malkemus, D., Perkins, R.B., Palmer, C.D., 2021. Geochemistry and geothermometry of Breitenbush Hot Springs, Oregon, USA. *Geothermics* 95, 102134.
- Mariner, R.H., Presser, T.S., Evans, W.C., 1993. Geothermometry and water—rock interaction in selected thermal systems in the cascade range and modoc plateau, western United States. *Geothermics* 22(1), 1-15.
- Mattson, E., Smith, R.W., Neupane, G., Palmer, C.D., Fujita, K., McLing, T.L., Reed, D.W., Cooper, C., Thompson, V.V., 2015. Improved geothermometry through multivariate reaction-path modeling and evaluation of geomicrobiological influences on geochemical temperature indicators, INL/EXT-14-33959. Idaho National Laboratory.
- McCleskey, R.B., Chiu, R.B., Nordstrom, D.K., Campbell, K.M., Roth, D.A., Ball, J.W., Plowman, T.I., 2014. Water-Chemistry Data for Selected Springs, Geysers, and Streams in Yellowstone National Park, Wyoming, Beginning 2009. [https://gallery.usgs.gov/mission-areas/water-resources/science/water-chemistry-data-selected-springs-geysers-and-streams?qt-science\\_center\\_objects=0#qt-science\\_center\\_objects](https://gallery.usgs.gov/mission-areas/water-resources/science/water-chemistry-data-selected-springs-geysers-and-streams?qt-science_center_objects=0#qt-science_center_objects).
- Michard, G., Roekens, E., 1983. Modelling of the chemical composition of alkaline hot waters. *Geothermics* 12(2), 161-169.
- Neupane, G., Baum, J.S., Mattson, E., Mines, G.L., Palmer, C.D., Smith, R.W., 2015. Validation of Multicomponent Equilibrium Geothermometry at Four Geothermal Power Plants, Proceedings, Fortieth Workshop on Geothermal Reservoir Engineering. Stanford University, Stanford, California, January 26-28, 2015, SGP-TR-204, 17p.
- Neupane, G., Mattson, E., Cannon, C., Atkinson, T., McLing, T., Wood, T., Worthing, W., Conrad, M., 2016a. Mixing Effects on Geothermometric Calculations of the Newdale Geothermal Area in the Eastern Snake River Plain, Idaho, PROCEEDINGS, 41st Workshop on Geothermal Reservoir Engineering Stanford University, Stanford, California, February 22-24, 2016 SGP-TR-209.
- Neupane, G., Mattson, E., Cannon, C., Atkinson, T., McLing, T., Wood, T., Worthing, W., Dobson, P., Conrad, M., 2016b. Potential Hydrothermal Resource Areas and Their Reservoir Temperatures in the Eastern Snake River Plain, Idaho, PROCEEDINGS, 41st Workshop on Geothermal Reservoir Engineering Stanford University, Stanford, California, February 22-24, 2016 SGP-TR-209.
- Neupane, G., Mattson, E., McLing, T., Palmer, C.D., Smith, R.W., Wood, T.R., 2014. Deep Geothermal reservoir temperatures in the Eastern Snake River Plain, Idaho using multicomponent geothermometry, Proceedings, Thirty-ninth Workshop on Geothermal Reservoir Engineering. Stanford University, Stanford, California, February 24-26, 2014 SGP-TR-202.
- Neupane, G., Mattson, E.D., McLing, T.L., Palmer, C.D., Smith, R.W., Wood, T.R., Podgorney, R.K., 2016. Geothermometric evaluation of geothermal resources in southeastern Idaho. *Geothermal Energy Science* 4(1), 11-22.
- Nordstrom, D., Jw, B., McCleskey, R., 2005. Ground water to surface water: Chemistry of thermal outflows in Yellowstone National Park, in: Inskeep, W.P., McDermott, T.R. (Eds.), *Geothermal biology and geochemistry in Yellowstone National Park : proceeding of the Thermal Biology Institute workshop*, Yellowstone National Park, WY, October 2003, 1st ed. ed. . Montana State University Publications, Bozeman, MT, pp. 73-94.
- Nordstrom, D., McCleskey, R., Ball, J., 2019. Thermal water chemistry of Yellowstone National Park after 24 years of research. *E3S Web of Conferences* 98, 07020.
- Palandri, J.L., Reed, M.H., 2001. Reconstruction of in situ composition of sedimentary formation waters. *Geochimica et Cosmochimica Acta* 65(11), 1741-1767.
- Palmer, C.D., 2014. Reservoir Temperature Estimator (RTEst) User Manual. Idaho National Laboratory, p. 46.
- Palmer, C.D., Ohly, S.R., Smith, D.J., Neupane, G., McLing, T., Mattson, E., 2014. Mineral selection for multicomponent equilibrium geothermometry. *Geothermal Resources Council Transactions* 38, 453-459.
- Pang, Z.-H., Reed, M., 1998. Theoretical Chemical Thermometry on Geothermal Waters: Problems and Methods. *Geochimica et Cosmochimica Acta* 62(6), 1083-1091.

- Parry, W.T., Bowman, J.R., 1990. Chemical and stable isotopic models for boundary creek warm springs, southwestern Yellowstone National Park, Wyoming. *Journal of Volcanology and Geothermal Research* 43(1-4), 133-157.
- Parry, W.T., Chapman, D.S., Bowman, J.R., Allis, R.G., 1981. Quantitative Assessment of Thermal Features of the Southwest Portion of Yellowstone Park. *Yellowstone NP Report* 5, 120-127.
- Peiffer, L., Wanner, C., Spycher, N., Sonnenthal, E.L., Kennedy, B.M., Iovenitti, J., 2014. Optimized multicomponent vs. classical geothermometry: Insights from modeling studies at the Dixie Valley geothermal area. *Geothermics* 51(0), 154-169.
- Powell, T., Cumming, W., 2010. Spreadsheets for geothermal water and gas geothermometry, Proceedings, Thirty-Fifth Workshop on Geothermal Reservoir Engineering. Stanford University, Stanford, California, February 1-3, 2010 SGP-TR-188, p. 10.
- Reed, M., Spycher, N., 1984. Calculation of pH and mineral equilibria in hydrothermal waters with application to geothermometry and studies of boiling and dilution. *Geochimica et Cosmochimica Acta* 48(7), 1479-1492.
- Reed, M.H., 1982. Calculation of multicomponent chemical equilibria and reaction processes in systems involving minerals, gases and an aqueous phase. *Geochimica et Cosmochimica Acta* 46(4), 513-528.
- Reed, M.H., 1998. Calculation of simultaneous chemical equilibria in aqueous-mineral-gas systems and its application to modeling hydrothermal processes., in: Richards, J., Larson, P. (Ed.) *Techniques in Hydrothermal Ore Deposits Geology, Reviews in Economic Geology*. pp. 109-124.
- Schwartz, G.M., 1959. Hydrothermal alteration. *Economic Geology* 54, 161-183.
- Shervais, J., Glen, J., Nielson, D., Garg, S., Liberty, L., Siler, D., Dobson, P., Gasperikova, E., Sonnenthal, E., Neupane, G., Deangelo, J., Newell, D., Evans, J., Snyder, N., 2017. Geothermal Play Fairway Analysis of the Snake River Plain: Phase 2. *GRC Transactions* 41, 2328-2345.
- Shervais, J., Glen, J., Siler, D., Deangelo, J., Liberty, L., Nielson, D., Garg, S., Neupane, G., Dobson, P., Gasperikova, E., Sonnenthal, E., Newell, D., Evans, J., Snyder, N., Mink, L., 2018. Provisional Conceptual Model of the Camas Prairie (ID) Geothermal System from Play Fairway Analysis, PROCEEDINGS, 43rd Workshop on Geothermal Reservoir Engineering, Stanford University, Stanford, California, February 12-14, 2018 SGP-TR-21.
- Shervais, J.W., Glen, J.M., Liberty, L.M., Dobson, P., Gasperikova, E., Sonnenthal, E., Visser, C., Nielson, D., Garg, S., Evans, J.P., Siler, D., 2015. Snake River Plain Play Fairway Analysis—Phase 1 Report. *GRC Transactions* 39, 761-769.
- Shervais, J.W., Glen, J.M.G., Siler, D.L., Liberty, L., Nielson, D., Garg, S., Dobson, P., Gasperikova, E., Sonnenthal, E., Newell, D., Evans, J.E., DeAngelo, J., Peacock, J.R., Earney, T.E., Schermerhorn, W.D., Neupane, G., 2020. Play fairway analysis in geothermal exploration: The Snake River plain volcanic province. PROCEEDINGS, 45th Workshop on Geothermal Reservoir Engineering Stanford University, Stanford, California, February 10-12, 2020 SGP-TR-216.
- Spycher, N., Peiffer, L., Sonnenthal, E.L., Saldi, G., Reed, M.H., Kennedy, B.M., 2014. Integrated multicomponent solute geothermometry. *Geothermics* 51(0), 113-123.
- Tole, M.P., Ármannsson, H., Zhong-He, P., Arnórsson, S., 1993. Fluid/mineral equilibrium calculations for geothermal fluids and chemical geothermometry. *Geothermics* 22(1), 17-37.
- Truesdell, A.H., Fournier, R.O., 1977. Procedure for estimating temperature of a hot-water component in a mixed water by using a plot of dissolved silica versus enthalpy. *Journal of Research of the U.S. Geological Survey* 5, 49-52.
- U.S. Department of Energy, 2011. Exploration Technologies, Technology Needs Assessment, Energy Efficiency and Renewable Energy, Geothermal Technology Program, DOE/EE-0663.
- Verma, S.P., Pandarinath, K., Santoyo, E., 2008. SolGeo: A new computer program for solute geothermometers and its application to Mexican geothermal fields. *Geothermics* 37(6), 597-621.
- White, D.E., Brannock, W.W., Murata, K.J., 1956. Silica in hot-spring waters. *Geochimica et Cosmochimica Acta* 10(1), 27-59.
- White, D.E., Fournier, R.O., Muffler, L.J.P., Truesdell, A.H., 1975. Physical results of research drilling in thermal areas of Yellowstone National Park, Wyoming, Professional Paper, - ed.

- Whitney, D.L., Evans, B.W., 2010. Abbreviations for names of rock-forming minerals. *American Mineralogist* 95(1), 185-187.
- Williams, C.F., Reed, M.J., Mariner, R.H., 2008. A Review of Methods Applied by the U.S. Geological Survey in the Assessment of Identified Geothermal Resources. U.S. Geological Survey, p. 30 p.
- Wolery, T.J., 1979. Calculation of chemical equilibrium between aqueous solution and minerals: the EQ3/6 software package. California Univ., Livermore (USA). Lawrence Livermore Lab. UCRL-52658, TRN: 79-010364, p. 46.
- Wood, T.R., Worthing, W., Cannon, C., Palmer, C.D., Neupane, G., McLing, T., Mattson, E., Dobson, P.F., Conrad, M., 2015. The Preston Geothermal Resources; Renewed Interest in a Known Geothermal Resource Area, Proceedings, Fourtieth Workshop on Geothermal Reservoir Engineering. Stanford University, Stanford, California, January 26-28, 2015, SGP-TR-204, 14p.
- Zimmer, K., Zhang, Y., Lu, P., Chen, Y., Zhang, G., Dalkilic, M., Zhu, C., 2016. SUPCRTBL: A revised and extended thermodynamic dataset and software package of SUPCRT92. *Computers & Geosciences* 90, 97-111.